Technical report; TR-208

KNMI

The KNMI Garderen Experiment, Micro-meteorological observations 1988-1989 Instruments and data set

F.C. Bosveld, J.G. van der Vliet and W.A.A. Monna

Koninklijk Nederlands Meteorologisch Instituut

De Bilt, 1998

Technical report = technisch rapport; TR - 208

De Bilt, 1998

PO Box 201
3730 AE De Bilt
Wilhelminalaan 10
De Bilt
The Netherlands
Telephone + 31(0)30-220 69 11
Telefax + 31 (0)30-221 04 07

Authors: F.C. Bosveld, J.G. van der Vliet (retired) and
W.A.A. Monna

UDC: 551.584.4
551.506.24
(492)

ISSN: 0169-1708

ISBN: 90-369-2143-0

The KNMI Garderen Experiment,

Micro-meteorological Observations 1988 - 1989.

Instruments and data set

F.C. Bosveld

J.G. van der Vliet

W.A.A. Monna

Contents

1 Introduction

In 1985 a start was made with ACIFORN (Acidification of Forests in the Netherlands), a sub-project of the Dutch Additional Programme on Acidification (Schneider and Bresser, 1986). The aim of ACIFORN was to assess the impact of air-pollution on tree vitality and tree growth (Vermetten et al., 1986). Two Douglas fir stands were selected, one near Kootwijk and one near Garderen (Speulderbos). The two locations have a different vitality, Speulderbos being the most vital one. These two eco-systems were monitored during the period 1986-1990.

A number of Dutch institutes were involved in the monitoring programma. The department of Air Pollution of the Agricultural University of Wageningen (AUW) performed profile measuremetns of air pollution concentration and micro-meteorological quantities. "De Dorschkamp", Research Institute for Forestry and Urban Ecology took care of the tree physiological and tree growth measurements. The department of Forestry of the AUW performed tree root measurements. Chemical composition of soil, rain and throughfall were measured by the department of Soil Science and Geology of the AUW. The Laboratory of Physical Geography and Soil Science of the University of Amsterdam took care of the soil physics and hydrology. This group of institutes formed the basis of ACIFORN. In 1988 KNMI started with detailed micro-meteorological measurements involving eddy-correlation measurements of momentum, heat and water vapour. At the same time ECN and TNO-MT became involved with more detailed air-pollution measurements. In 1989 KEMA performed xylem sapflow measurements and the University of Amsterdam performed micro-wave canopy water storage measurements.

The main objective of the KNMI contribution to ACIFORN was to determine flux-profile relations for heat and momentum and to develop an algorithm for the derivation of air-pollution deposition fluxes from concentration gradient observations. This also involved an assessment of the influence of limited fetch on the derived surface fluxes. More generally KNMI is interested in the behaviour of the components of the surface energy balance over various kinds of vegetations.

In January 1988 a 36 m tall mast was erected at the Speulderbos site. Instrumentation and testing took the next three month. The first measuring campaign was held during the month of May. In the summer we had great problems with a mice plague which had invaded vital amplifiers of the measuring system. During the month of September the next campaign was held. The winter period 1988-1989 was used for evaluation of the data. During the period March 30st 1989 till January 10th 1990 the measuring system was operated almost continuously.

During the growing season of 1989 a number of auxillary measurements were performed by various groups. From the collaboration during this period a new project group emerged, CORRELACI (CORRELation of ACIforn results), in which KNMI participated. This group has tried to integrate the data-sets of the different disciplines around the central question of the influence of natural and artificial stress factors on the cycles of carbon,

nutrients and water (Evers et. al, 1991).

This report documents the KNMI field experiment at the Speulderbos location during 1988 and 1989. It describes the forest, the measuring tower, the data acquisition system and the database. It gives detailed information on instruments and their calibration. Corrections are described if they can be applied from the literature, or if they can be straight forwardly derived from the measurements and calibration results. Corrections which involve a more detailed analysis will be described else where.

2 Experiment

2.1 Location

The experimental site is located 2 km north of the village Garderen in the north-west part of the Veluwe, in the centre of the Netherlands as indicated in figure 1a. The geographical coordinates are 52°15'N, 5°41'E. The terrain is situated at 52m above mean sea level. The site is situated in an extended area of forest. Figure 1b shows the extension of the forest. The nearest edge of the forest is in easterly direction at a distance of 1.5 km. Figure 1c shows the pattern of the nearby stands together with height contours. The forest consists of small stands of a few hectares of different tree species with different heights. The nearest stands consists of Japanese Larch (to the north), Scotch Pine (to the west and south) and Beech (to the east). The north site of the stand borders partly on a clearing. Tree height varies a few meters between stands, being highest in westerly directions and lowest in southerly directions. In the easterly directions no tree height jumps occur in the first few hundred meters.

The forest stand in which the research station is situated consists of 2.5 ha of Douglas Fir (*Pseudotsuga menziesii*) planted in 1962. In 1989 the tree height varied between 15 and 20 m, averaged height was 18m. Tree growth is about 0.5m per year. Tree density is 785 trees/ha. The average tree diameter at breast height (DBH) is 20 cm. For a detailed biometrical description of the stand see Evers et al. (1990). The forest floor consists of a humus layer of 5 cm thickness. The soil consists of heterogeneous sandy loam to loamy sand textured ice pushed river sediments. The ground water table is at 40 m beneath the forest floor. No capillary uprise of ground water to the root zone can occur. Water holding capacity in the root zone ranges from 5 to 10 cm. For detailed information on the soil characteristics of the site see Tiktak and Bouten (1990).

2.2 The research station

Mast

A 36 m mast is guyed on three sides at three levels, 36, 24 and 12m. Guys are attached to ground anchors in the forest floor, two anchors for each guy. Figure 2a shows the mast configuration. The mast has a triangular basis with sides of 1.2m and consists of 6 identical segments. Climbing is done on the inside. At each measuring level (4, 18, 24, 30 and 36m) there is a working platform inside the mast. Cup anemometers are mounted at 3m and psychrometers at 2.5m from the centre of the mast on booms that can be rotated along side the mast for maintenance. The four booms above the forest point to 187° azimuth. The boom at 4m above the forest floor points to 90° azimuth. The fast response sensors including the quite heavy sonic anemometer equipment are mounted at 2.8m from the centre of the mast on a separate boom that can slide in a horizontal direction for main-

A

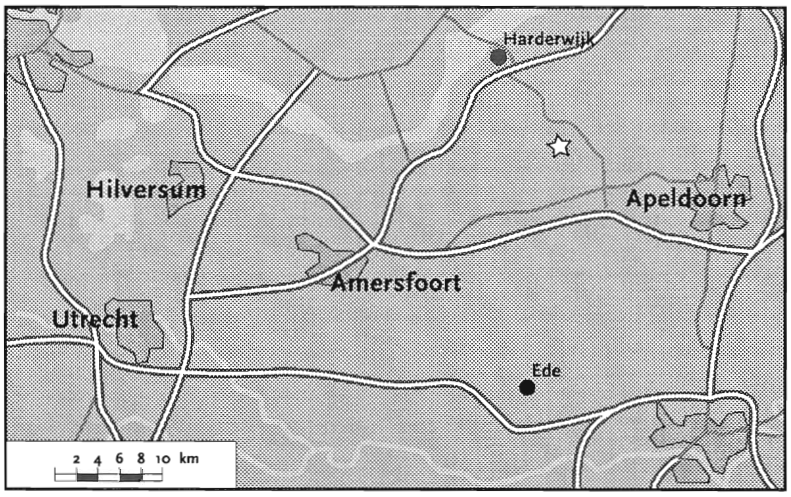
Harderwijk
Hilversum
Apeldoorn
Amersfoort
Utrecht
Ede
2 4 6 8 10 km

B

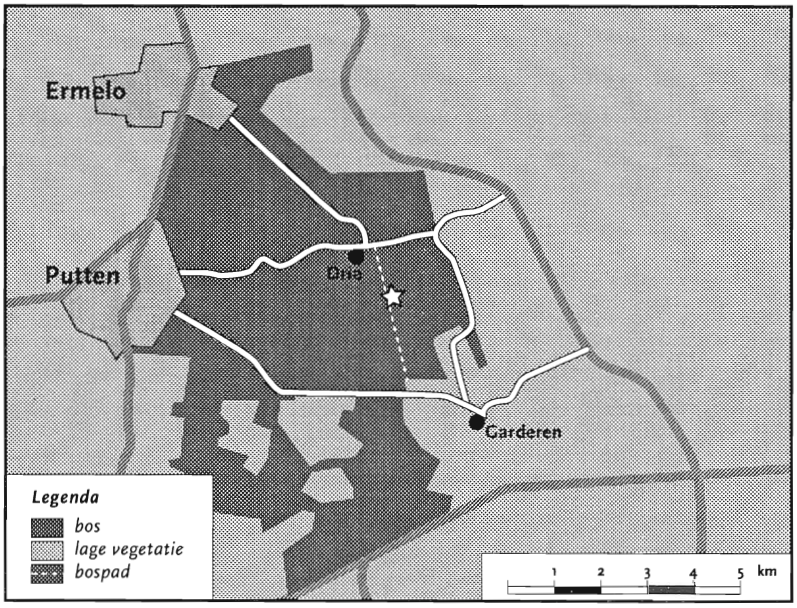
Ermelo
Putten
Dria
Garderen
Legenda
bos
lage vegetatie
bospad
1 2 3 4 5 km

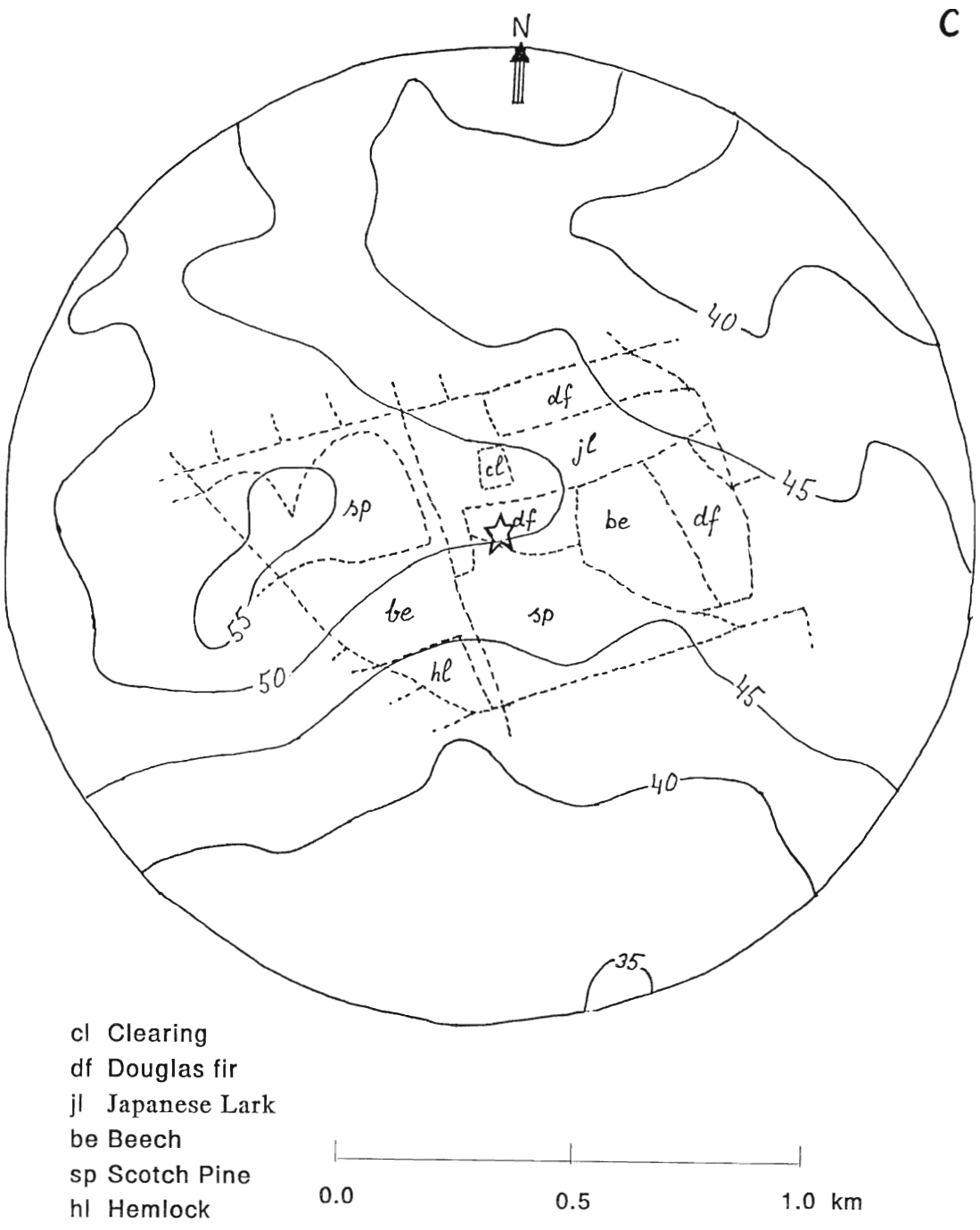

Figure 1 a) Location of the research site Speulderbos (indicated by white star), b) extension of the forested area, c) Pattern of the nearby stands.

tenance. This boom points to 180°. A net radiation meter is placed at a boom in the top of the mast at 3m from the centre of the mast in a 120° direction from north. Figure 2b shows the configuration in the top of the mast. The lightning conductor is situated such that no shading can occur on the shortwave incoming radiation instrument and the net radiometer.

With respect to flow obstruction of the mast an estimation of wind speed disturbance is made on the basis of Wessels (1983). An effective diameter for potential flow of 0.3m is calculated. This induces an error of 1.5% in the wind speed for a wind direction perpendicular to the arm.

Due to improper dimensioning of the floor plate at the foot of the mast the mast sank gradually deeper into the forest floor. The guy tension was measured regularly and when necessary the guys were restrained. After one year this sinking had stopped. The depth by then was about 0.2m. No corrections are made for this. To prohibit rotation of the mast along a vertical axis a horizontal beam was stiffly connected to the mast at 1 m height and fixed in the forest floor.

Main supply was obtained from the regular 220 Volt electrical power line. The connection is galvanically separated by a 1:1 transformer. A low resistance connection to ground potential is essential for good performance of the electronics and for protection against lightning. Since the ground water table is at 40m below the forest floor long electrodes are needed. The disadvantage of long electrodes is that by self induction, quickly changing current induce high electrical voltages. Therefore two types of electrodes were used. Long ones to provide a good electrical ground during normal operation and several shorter electrodes to spread electrical current over a larger area when induction by lightning occur. The grounding consists of 3 electrodes down to 40 m depth connected to the tree outer guys, 6 electrodes to 9 m depth connected to the six inner guys and 3 electrodes to 30m depth connected to the foot of the mast. The total resistance of the grounding system is about 5 Ohm.

Protection of the signal lines against lightning is done with gas tubes, VDR's and tranzorbs. The thermocouples are not protected with semi-conductors since the resistance to ground has to be larger than 5 MOhm. As far as we know there has never been a direct strike by lightning during the whole experiment. On a few occasions the computer system stopped, possibly due to induction current during lightning.

Instruments

Cables from the instruments in the mast are led downward to a van circa 30 m south of the mast. In this van electronics and the computer are placed. The van is kept at a temperature above 15°C to avoid moisture formation in the equipment.

The instruments can be divided in two classes. The fast response instruments are used for measuring the turbulent fluctuations of wind, temperature and water vapour. From these measurements the eddy-correlation fluxes are derived. The slow response instruments involve dry- and wet bulb sensors, wind speed, wind direction and radiation sensors. Table 1 gives the heights of the temperature and wind instruments. The levels are numbered

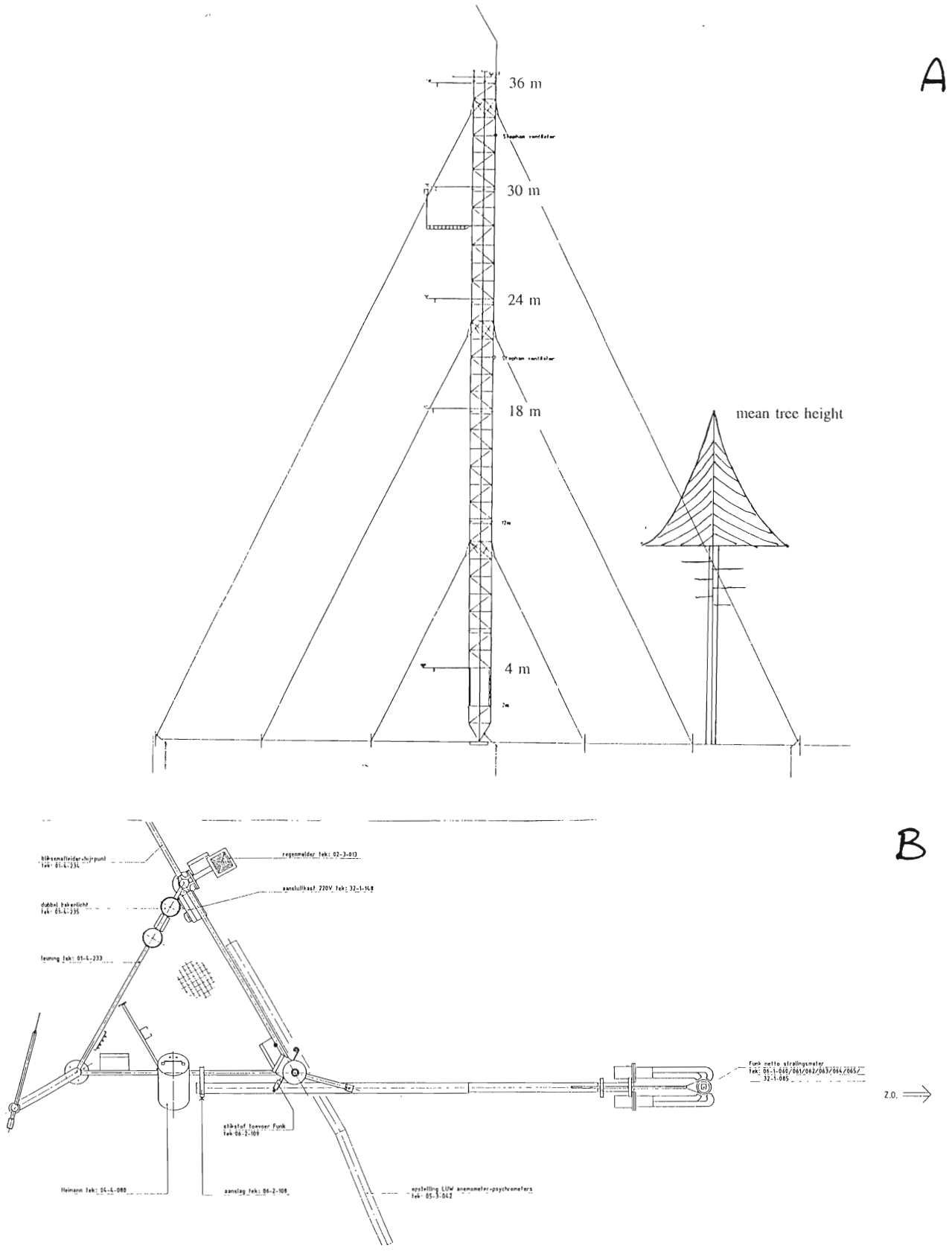

Figure 2 a) The 36m high guyed mast, b) Downward view at the top of the mast.

Table 1 Height of the instruments above the foot of the mast in meters

Level	Temperature	Wind-cups	Sonic
0	3.71	4.16	
1	17.67	18.12	
2	23.67	24.12	
3	30.51	30.96	29.67
4	35.49	35.94	

from 0 to 4. In table 2 the instruments are listed together with their manufacturer and the level numbers where they are mounted in the mast. Table 3 lists the accuracy of the instruments together with the resolution.

2.3 Data sampling and processing

Data are sampled with a 12 bits A/D converter in the range of -5 to +5 Volt. This corresponds to a resolution of 2.5 mV. The data are collected with a Digital PDP11-system with a sample rate of approximately 1 s. Mean values, standard deviations and correlations are calculated on-line on a 10 minute basis. Structure parameters of turbulent quantities are stored occasionally. For a definition see eq.(18). The reduced data are stored on disk. Collected data of were transmitted to a cassette tape (later to a PC-floppy disk) each week. Afterwards the data are screened for instrumental malfunctioning. The final data-set consists of half hour mean values and is supplemented with essential quantities derived from the basic data. The 10 minute averaging serves as a crude detrending filter for the covariances. The half hour time is chosen to give a well defined average especially for the covariances.

2.4 Maintenance

During normal operation the instruments were checked each week. This check includes cleaning the radiation and temperature sensors and filling water into the water supply cans of the wet-bulb sensors.During special campaigns when the Pt-wire and/or Ly-α were operated the instruments were checked more often.

2.5 Measuring periods

Most instruments were operated during two campaigns in 1988 and during most of the year 1989. The periods are listed in table 4. Some instruments were operated only during shorter periods. The Pt-50 cold wire temperature sensor was operated during most of the 1988 campaigns and in 1989 during periods in April 1989. The Ly-α Hygrometer was also operated during most of the 1988 campaigns and during approximately 50 days in 1989. During the April-May 1988 campaign no structure parameters were measured except with

the scintillometer. The September measurements contain structure parameters of temperature, humidity and wind both horizontal (A and B sensor of sonic anemometer) as vertical (W) together with the scintillometer signal. In the period 5-12 september a software error in transforming the horizontal wind components of the sonic anemometer obstructed the output. The data were corrected afterwards. In 1989 no scintillometer measurements were performed. Structure parameters of the vertical wind were registrated during the whole year. Humidity structure parameters are present when the Ly—α was in operation.

Table 2 Instruments, manufacturer and their position in the mast

Instrument	Manufacturer	Level
Fast response		
1 Sonic anemometer thermometer	Kaijo Denki	3
1 Pt-wire thermometer	KNMI	3
1 Ly-a Hygrometer	ERC	3
Slow response		
5 Cup anemometers	Agr.Un.Wageningen	0,1,2,3,4
5 Cu/Co Thermocouples (dry bulb)	KNMI	0,1,2,3,4
5 Cu/Co Thermocouples (wet bulb)	KNMI	0,1,2,3,4
2 Pt-500 resistance thermometers	KNMI	0,1
1 Wind vane	KNMI	4
1 Global radiation	Kipp CM11	4
1 Infrared thermometer	Heimann KT-24	4
1 Net radiation	Middleton (Funk type)	4
1 Scintillometer	KNMI	4
1 Rain indicator	ECN	4
1 Barograph	Fuess	in van
1 Precision aneroid barometer	Negrettie & Zambra	in van

Table 3 Characteristics of the instruments and their A/D conversion.

Instrument	Units	Calibration in Units/Volt	Accuracy	Resolution of instrument	Resolution A/D conversion
Horizontal wind sonic	m/s	5	1%	0.005	0.013
Vertical wind sonic	m/s	1	1%	0.005	0.0025
Temperature sonic	K	10	1%	0.025	0.025
Cup anemometer	m/s	5	0.05	0.125	0.013
Absolute temperature	K	10	0.2	<0.05	0.025
Thermocouple large difference	K	5	0.02	<0.005	0.013
Thermocouple small difference	K	1	0.02	<0.005	0.0025
Global radiation	W/m^2	500	1 %	1	1.3
Net radiation	W/m^2	400	5 %	1	1.0
Radiation temperature	K	7	1	0.25	0.0175
Wind vane	degree	108	3	1.5	0.25
Rotor	degree	100	3	1	0.25
Inclinometers	degree	5	0.05	0.02	0.013

3 Wind measurements

3.1 Cup anemometer

Vertical wind gradients over an aero-dynamical rough vegetation like forest are likely to be very small. Usually wind differences between the subsequent levels of the profile are 0.5 to 1.0 m/s. For an accuracy of 5% in the derived flux-profile relations we thus need an absolute accuracy of 2.5 to 5 cm/s in the wind speed differences. Consequently special care has to be taken by the calibration.

Instrument specifications

Wind speeds are measured with cup-anemometers fabricated at the Agricultural University of Wageningen (the Netherlands), and generously made available for this experiment.

Specifications:

Mechanical : Three conical cups

Cup diameter	= 0.050 m
Arm length	= 0.030 m
Radius to cup centre	= 0.055 m

Electrical : Photo-chopper 4 pulses per rotation

Performance: Response length l_o = 1.4 m/s.

Table 4 Periods of operation.

Begin	End	Remarks
26-Apr-1988	29-Apr-1988	Normal operation
3-May-1988	12-May-1988	Normal operation
12-May-1988	18-May-1988	Test thermo-couples
5-Sep-1988	12-Sep-1988	Normal operation
15-Sep-1988	18-Sep-1988	Test wet profile dry
19-Sep-1988	22-Sep-1988	Normal operation
26-Sep-1988	1-Oct-1988	Normal operation
30-Mar-1989	10-Jan-1990	Normal operation

Threshold-sensitivity	= 0.3 m/s.
Calibration coefficient	= 1.16 m/cycle
Elevation response parameter μ_2	= 1.0

The cup anemometer pulses are counted on the up and down going edge of the photo chopper signal and counted over a period of 1.16 s. This count is fed into a 8 bit D/A converter. The passage of 1.16m of air corresponds to one cycle of the cup anemometer. Thus a wind speed of 1 m/s gives a count of 8. The resolution then is 0.125 m/s. The maximum wind speed that can be counted is 32 m/s. 1 Volt output corresponds to 5 m/s, thus the 2.5 mV resolution of the data registration A/D converter corresponds to 1.25 cm/s. From the 5 Volt range of the A/D-converter we derive a maximum of 25 m/s that can be registrated. The D/A conversion factors stayed stable over the measuring period within 0.1%.

Operation and Maintenance

The seven cup anemometers were labelled nr 3 - 9. Table 5 shows the order in which the instruments were mounted. Cup-anemometer nr 3 was never in operation. Cup-anemometer nr. 5 was found with a tilted cup in November 1988 and repaired in March 1989. Cup-anemometer nr. 7, the cups though not tilted, appeared to be untied and were repaired also in March 1989. A very small tear was found in one cup of nr. 7. It was assumed that this had no effect on the calibration.The cup anemometers were in operation during the periods March until October 1988 and March 1989 until January 1990.

Calibration and accuracy

Calibration was performed at the wind tunnel of the Department of Meteorology of the Agricultural University of wageningen before the start of the experiment. Subsequently a number of calibrations were performed at the wind tunnel of KNMI (Monna, 1983). Table 6 lists the successive calibration dates of the cup-anemometers. At each occasion all cup anemometers were calibrated. At the KNMI calibration laboratory wind calibration data were plotted and interpolated to whole m/s number wind speeds. This is accurate enough for use in the meteorological network in which an accuracy of 0.5 m/s is desired. Here the desired accuracy is higher. For calibration II the original data could be read from graphical plots with limited precision. For calibration III no original data could be traced and thus was rejected from the analysis. For calibration IV and V the original data were available. Calibration IV was performed to check the reproducibility of the calibration procedure. During the whole experiment no further maintenance was performed on the cup anemometers.

Figure 3 shows calibration V relative to a reference linear curve $U = 0.294 \cdot f + 0.17$ (m/s) for the cup numbers 3, 4, 6, 7, 8 and 9, where f is the number of pulses per second (not doubled). It is observed that the individual calibrations are not linear.

A second order regression was performed on the calibration data. To render regression coefficients statistically independent an expansion on the basis of Legendre polynomes on the interval 0-70 pulses/sec was used. This interval corresponds to a wind speed interval of 0-20 m/s. The Legendre polynomes were scaled such that the regression coefficients are a

Table 5 Order of cup anemometer mounting in the mast

Level	Cup nr
4	6
3	7
2	8
1	5 (from 30-Mar-1989 nr 4)
0	9

direct measure of the contribution to the explained variance. The three regression coefficients are defined by:

$$U_{ref} = a_0 + a_1 \sqrt{3}\left(\frac{f}{35} - 1\right) + a_2 \sqrt{5}\left(\left(\frac{f}{35} - 1\right)^2 - \frac{1}{2}\right) \quad (1)$$

In figure 4 the coefficients a_0, a_1 and a_2 of the three remaining calibrations at KNMI (II, IV and V) are plotted for each cup-anemometer. It is observed that the subsequent calibrations show common deviations for all cup anemometers. This is particularly so for the two latest calibrations for which the most accurate results were available. It is not clear what the reason for this behaviour is. A possibility is aging of the cup anemometers, however, since the number of rotations during the measuring period are quit different for the different anemometers this is not likely. Another possibility is that there is a non-reproducible factor in the calibration procedure, although special care has been taken to position the cups always at the same position in the wind tunnel test section. Whatever the reason for this trend might be, it is encouraging to see that the trend is about the same for all the cup-anemometers. In the original data set only a linear regression curve was used. Wind data are corrected with the second order calibration obtained by averaging calibration IV and V. For profile measurements the accuracy of the wind differences in the profile is of special importance. Inspection of the regression coefficients and the individual calibration data indicate that the error in the wind differences is of the order of 5 cm/s. Comparing calibration I performed in the LUW wind tunnel with the calibration in the KNMI wind tunnel results in a difference of 5% in the absolute wind speed.

Stalling

In the wind tunnel the threshold sensitivity was measured. The wind speed was gradually increased until rotation of the cup anemometer started. For all the cup anemometers this threshold increased somewhat as time passed. However this value was always found lower then 0.5 m/s and most of the time between 0.25 and 0.30 m/s. Since only 10 minute averages are retained in the data set stalling can not be detected in the data-set. Thus 10 minute values lower then 1.0 m/s are probably in error.

Overspeeding

A treatment of overspeeding corrections is given in Bosveld (1997). It involves an analysis of the typical turbulent characteristics of the roughness layer over the forest. Here we describe the instrumental characteristics that need to be known for performing overspeeding corrections. They are the response length l_0 and the elevation response parameter μ_2.

The response length is determined in the wind tunnel from the e^{-1} response time τ to a step function in wind speed going from 0 to 2 m/s and from 0 to 4 m/s. This was achieved by blocking the cup anemometer with a thin wire after which the wire was suddenly released. For both steps a response length $d=U\tau$ of 1.4 m was found, where U is wind tunnel speed.

The elevation response is determined by tilting the instrument in the wind tunnel at a constant tunnel airspeed. Figure 5 shows $g(\vartheta)$, the wind speed sensed by the cup anemometer divided by the wind tunnel speed, as a function of elevation ϑ. Kristensen (1993) derives a relation between $g(\vartheta)$ and μ_2:

$$g(\vartheta) = \cos(\vartheta) + \frac{1}{2}\mu_2\vartheta^2 \qquad (2)$$

For an ideal instrument the elevation response is a cosine function. μ_2 is a measure for the deviation from the cosine response. For elevations up to 40° we derive from figure 5 $\mu_2=1.0$. Elevations larger then 40° are not dealt with here. These large elevations are rare in field experiments

3.2 Wind vane

Instrument specification

Wind direction was measured with the standard KNMI Vane. The resolution is limited to 1.5° due to a 8-bit code disk.

Table 6 Calibration date and location of the cup-anemometers.

Nr	Date	Location
I	Feb. 1988	AUW
II	Mar. 1988	KNMI
III	Nov. 1988	KNMI
IV	Mar. 1989	KNMI
V	Jan. 1990	KNMI

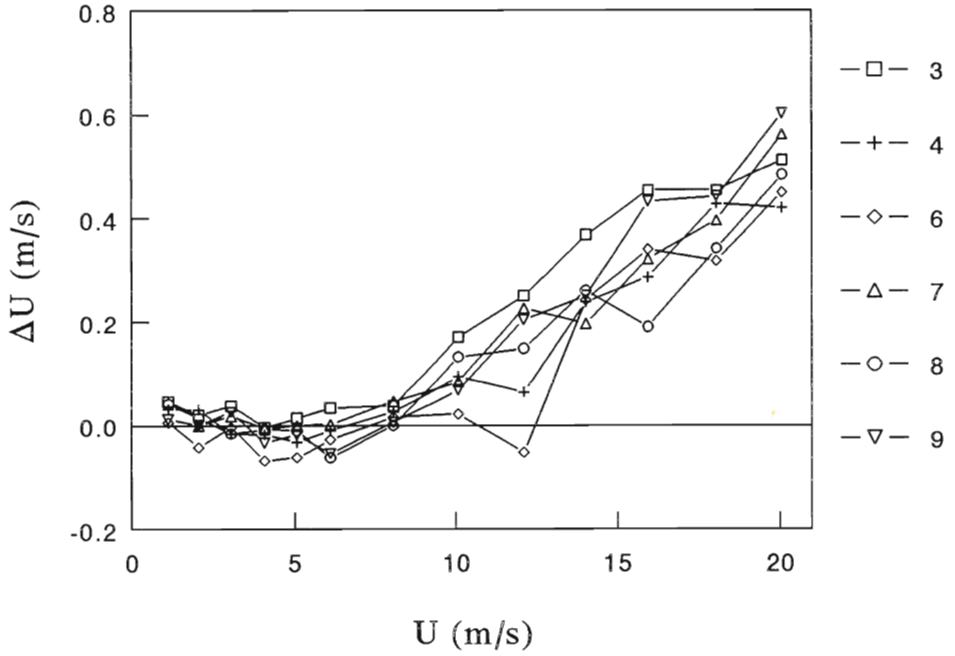

Figure 3 Calibration V relative to a reference calibration (U=0.2940*f+0.17 m/s) for cup nrs. 3,4,6,7,8 and 9.

Operation and maintenance

In the period March till November 1988 the vane with KNMI nr 01-00-524-39 was used. In March 1989 the vane was found with a malfunctioning code-disk. Also the vane blade itself was somewhat distorted. The vane was replaced by nr 01-00-524-52.

Calibration and Accuracy

The azimuth angle calibration of the instruments showed deviations of at most 0.4 degrees. No correction was made for this. The geographical direction of the instrument was measured in two ways. At the 25th of May 1988 the vane was fixed in one position. The direction of the vane was measured with a compass and a binocular from a distance in the field. From this it was found that the zero point was at +2° relative to north.

At the 28th of March 1989 a method of Slob (private communication) was used. With a special construction the vane was positioned exactly in the direction of the sun. This was done with a shading plate. The instrument reading was taken together with the exact time of reading. The solar angle was read from a nautical table. The zero point was found at -0.85° relative to north. From these tests we assume that the accuracy is 3°.

3.3 Sonic anemometer, inclinometer and rotator.

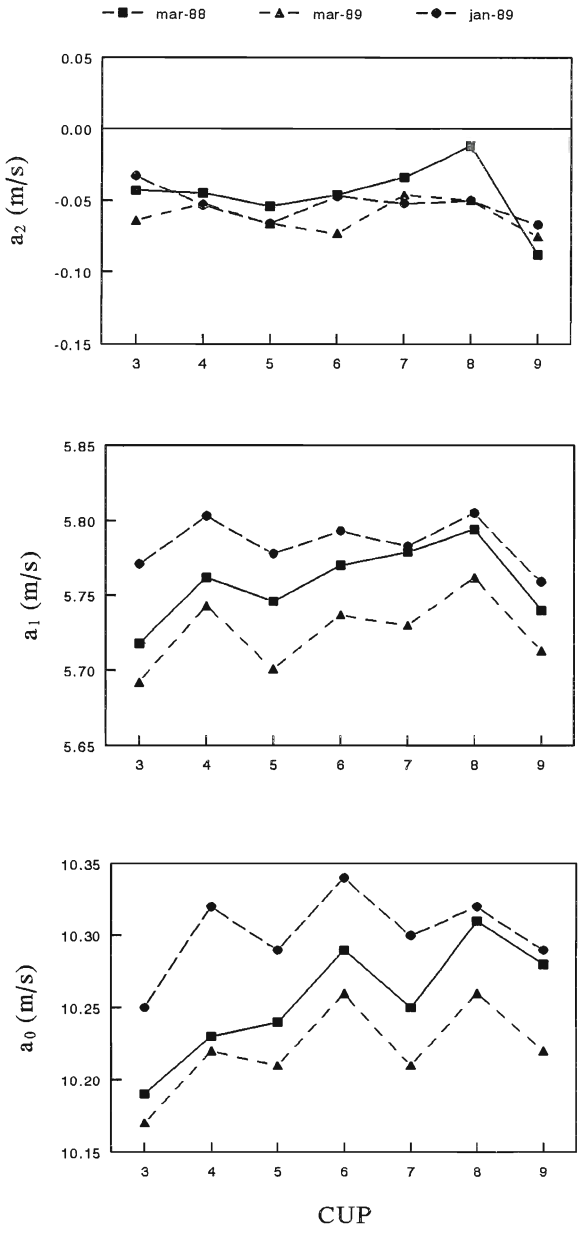

Figure 4 Second order regression results for the seven AUW cup anemometers. Coefficients refer to Legendre polynome expansion.

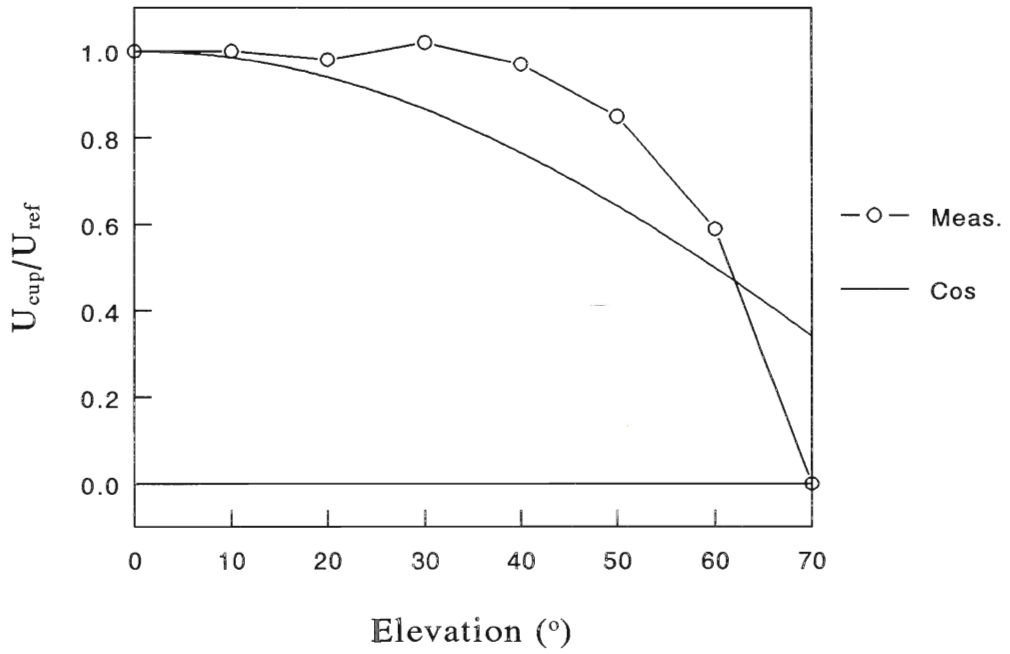

Figure 5 Elevation response of an AUW-cup anemometer.

instrument specification

The sonic anemometer used in this experiment is a Kaijo-Denki DAT-300 with probe type TR-61A. (KNMI numbers 01.00.017.xx; Probe xx=16, Junction box xx=12, Electronica unit xx=13)The instrument measures the three components of the wind speed by measuring the travel time of a sound pulse over a path of 0.2m. Wind speed is measured along a vertical path and along two horizontal paths under an angle of 120°. The instrument is extensively described by Schotanus (1982). The horizontal coordinate system is defined in figure 6. Here u is the horizontal wind vector. The signal of the A-sensor (ASON) and the B-sensor (BSON) are converted to the orthogonal components YSON (forward) and XSON (sideward) component by the datalogger software:

$$YSON = ASON + BSON$$
$$XSON = -\frac{1}{\sqrt{3}} \cdot (ASON - BSON) \qquad (3)$$

The vertical wind sensor gives for upward wind positive values.

Calibration and accuracy

The wind components are calibrated by a method described by Kraan and Oost (1989). Here we rely on a calibration of the instrument performed in 1993. From this calibration it

is deduced that the vertical sensor is tilted by 0.5° in the direction ϕ=-90° (see figure 8 for definition of tilt coordinate frame). Furthermore an error in the D/A converter was discovered and traced back to at least 1986. This error results in a jump at downward zero-crossing of the wind speed components of -0.14 cm/s. The consequences and corrections are discussed in Bosveld (1997). Zero shift is measured regularly by protecting the sound paths against wind by means of plastic tubes. Measurements are corrected for these shifts.

Rotator of sonic anemometer

The sonic anemometer is mounted on a rotator device manufactured at KNMI, which is electrically driven to turn the sonic into the wind. Turning is performed at each visit. The consequence is that a large fraction of the measurements are taken outside the azimuth range for which suitable corrections for wind speed and friction velocity can be made. It is believed that the influence of bad orientation on scalar fluxes is limited. The azimuth of the rotator is registrated parallel with the other signals. The zero point of the rotator azimuth is determined by observing the sonic from a suitable place in the field with a binocular. The line between the vertical sonic-sensor and the backside of the frame serves as an indication of the forward direction. With a compass and suitable corrections for the deviation between true and magnetic north pole the azimuth is determined. A definition of the coordinate system of the rotator azimuth is given in figure 7. Here ROTR is the azimuth of the rotator relative to North, DDSN is the wind direction relative to North.

Inclinometer

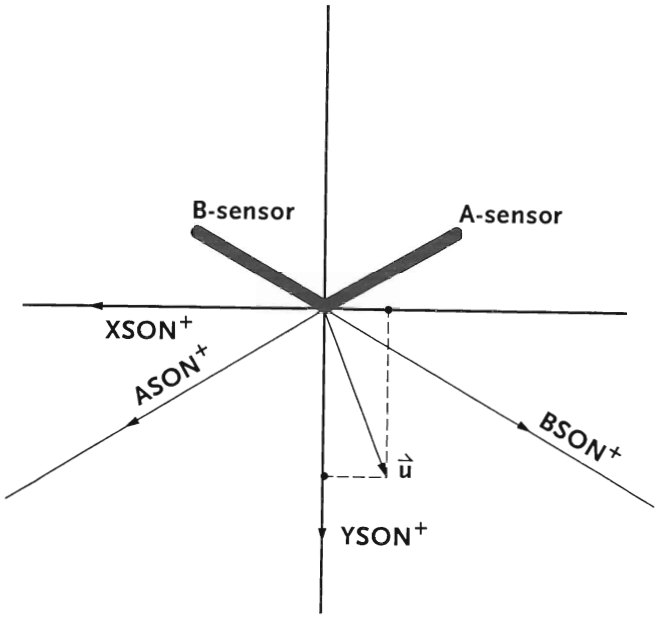

Figure 6 Coordinate system for the horizontal wind components.

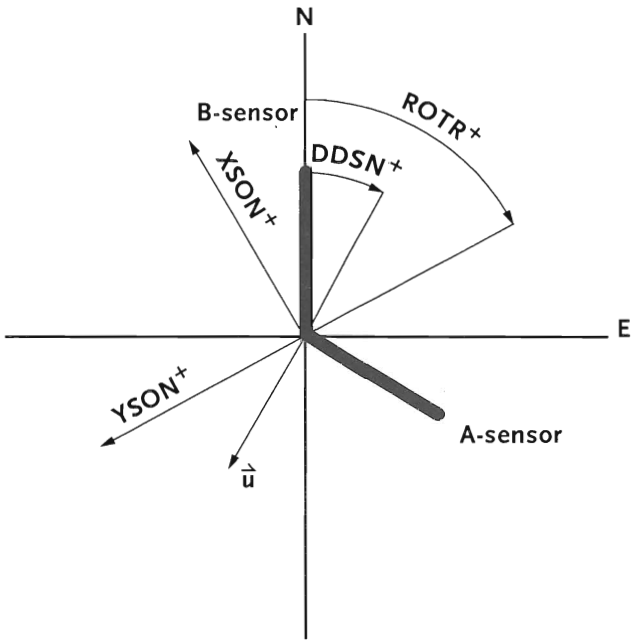

Figure 7 Coordinate system for the azimuths of rotator (ROTR) and sonic derived wind direction (DDSN).

The levelling of the Sonic anemometer is measured with an inclinometer mounted between the rotator and the stem. The thin 1 m long stem is used to avoid flow obstruction from the rather bulky inclinometer. Figure 8a gives the coordinate system of the inclinometer relative to the sonic probe. Here XWAT and YWAT are the two components of the inclination. XWAT is positive if the upperside of the sonic is rotated towards the $XWAT^+$ direction indicated in the figure. Figure 8b shows the same coordinate system extended with a polar coordinate system which is defined by the absolute rotation out of the horizontal plane (θ) and the azimuth of the direction of rotation (φ). In this figure it is shown how two rotation, the tilt of the vertical sonic wind sensor (tilt) and an arbitrary inclinometer rotation (inc) are composed to one rotation representing the total rotation of the vertical wind sensor relative to the horizontal frame. Each time the boom on which the fast response instruments were mounted was pulled in and out for maintenance the levelling of the sonic changed a bit. An inspection of the measurements shows that θ, varies between 0.4° and 0.8°, whereas φ which is the azimuth of the rotation relative to the fixed N-E frame, varies between 240° and 260° indicating. This indicates that the boom at which the sonic is mounted has an approximately fixed tilt.

frame of reference for the turbulent stress tensor

The orientation of the reference frame is especially important for the determination of the vertical turbulent fluxes, of which especially the stress (<uw>) is very sensitive to the definition of the vertical direction. In the forest situation where the surface is not level because of differences in tree height between the different stands and because of slightly sloping terrain there is some uncertainty which frame should be chosen. Uncertainty in the

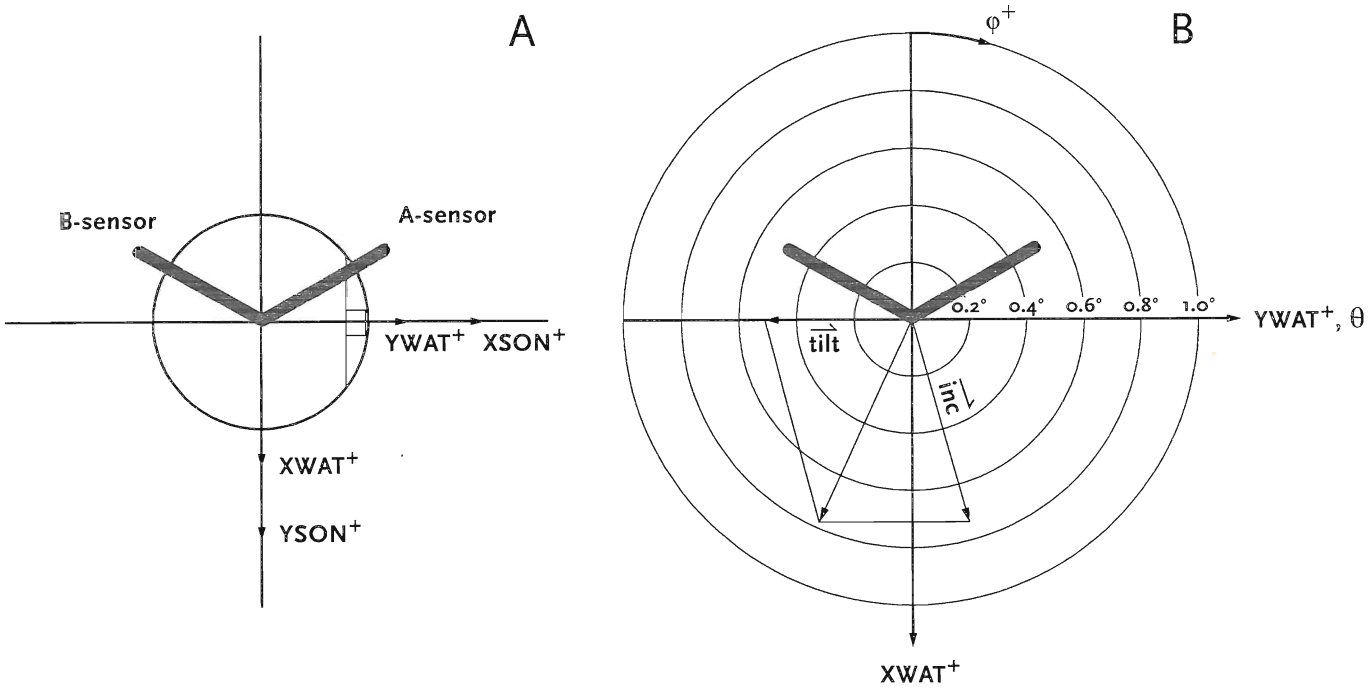

Figure 8 a) Orientation of inclinometer relative to sonic frame. b) Same as a but with polar coordinates and rotation vector summation, see also text.

orientation of the horizontal plane can give cross talk of the <uu> component (variance of the wind along the mean wind direction) into the <uw> component of the turbulent stress tensor. The variance of the horizontal wind is approximately 4 times larger than the stress and of opposite sign. For a tilt of the horizontal plane of 0.02 radial (1.2°) towards the mean wind direction we have an overestimation in |<uw>| of approximately 8%.

The orientation of the sonic anemometer probe has three degrees of freedom and is given by the two inclinometer components and the rotator azimuth angle. This defines a coordinate frame with the vertical axis parallel to the direction of gravity and a North-East frame in a plane perpendicular to the direction of gravity. If streamlines of the mean wind are not level there is some ambiguity in the way the reference frame should be defined. One method is to choose one axis along the average streamlines, defined by <W> = 0 and <V> = 0. The freedom of rotation along the streamline is often fixed by choosing <uv> = 0. This is convenient, because these quantities are available, but incorrect in principle because the covariance between the lateral and longitudinal wind fluctuations is not zero, even in level terrain, because of veering of the wind with height.

Another approach is to take as the lateral direction the direction perpendicular to the gravitational vector and perpendicular to the mean wind direction. Subsequently the vertical direction is defined as the direction perpendicular to this lateral direction and the mean windvector. This definition is correct for an infinite sloping terrain if we refrain from stability effects. Stability effects introduce inevitably a second vertical preference level. We cannot have it all. For the stress the difference between the two methods will be small because <uv> is small in both definitions.

Another point is whether the coordinate frame should be adjusted for each time interval or should be fixed for a longer period. Since the average vertical wind velocity over a certain time interval is subject to the random process of turbulence some extra noise is introduced. In other words, the true mean streamline is different from the mean streamline determined over a certain time interval. An estimation of the standard deviation of the mean vertical wind over a 30 minute interval can be given on the basis of Lumley and Panofsky (1964). At the height of 18 m above zero plane and with a wind speed of 4 m/s we have as integral time scale for the vertical wind of $0.4 \times 18/4 = 1.8$ sec. For an average over a half hour we have 1800/1.8 random experiments with each a standard deviation of 1 m/s say. This gives a standard deviation of 0.03 m/s in the mean vertical wind. This result in a random tilt of the streamlines of 0.0075 rad (0.3°) and consequently a random signal on the stress after tilt correction of 3%. A conceptual more appealing way is to determine the tilting of the streamlines for each wind direction. It then is assumed that this tilting depends only on wind direction. Turning of the frame of reference is then performed as a function of wind direction.

Although there are conceptual differences between the various solutions the results do not differ much. We decided to use the common method to rotate into the main wind. The rotation along the main wind vector axis is not performed since the sonic is already almost level and it has little consequence for the relevant components of the stress tensor. For study of the tilting of the streamlines however the vertical component of the main wind vector is calculated relative to the plane perpendicular to the gravitational vector.

4 Temperature and humidity

4.1 Thermocouple/Pt500 psychrometer system

Instrument specifications

The psychrometer system consists of two parts. One for the above forest profile and one for the inside forest level. Temperature differences are measured with Copper/Constantane thermo-couples, while two 4-wire Pt500 elements provide the thermo-couple reference to the absolute temperature. The Pt500 elements are thermally connected to the thermo-couples in an Aluminium block. The thermocouple chain above the forest is closed. This means that we can check the system by adding all temperature differences in the chain. By proper operation this should sum up to zero. The thermo-couples and their shielding is a modified version of the Cabauw type sensor as described by Slob (1978). The modifications consists of:

- different water supply through the sensor boom
- thicker sensor head
- wider inner shield.

The third modification was made to avoid water-bridges between sensor and inner shield, which frequently occurred with the original system. Indeed the problem seems to be solved. Possible changes in the heat-contamination effects as described by Slob (1978) for the old system is not tested for. This effect occurs when the wind speed approaches the ventilation speed which is approximately 9 m/s and since the wind velocity over the forest is generally quit low (< 5 m/s say) we assume that this effect is negligible for most of the time.

The wet-bulb sensors are provided with a cotton wick which is continuously wetted with demineralised water by means of a peristaltic pump.

Operation and maintenance

Each week the temperature system was cleaned and water tanks for the wet-bulb system were filled. Wicks were cleaned with a plant water spray device. When the wicks could not be cleaned any more. This occurred every 4 to 5 weeks. Care was taken that the sockets were flooded as described by Wylie and Lalas (1981) to avoid contamination by organic material.

During the whole experiment the same Pt500 elements were used, labelled "SPEULD LEVEL 0" and "SPEULD LEVEL 1" according to their position in the mast. The thermocouple elements with KNMI NR 01-02-08-XX were positioned according to table 7.

Table 7 Positioning of the thermo-couples in the mast.

Level	Dry Bulb	Wet Bulb
4	16	17
3	18	19 (from july 1989 nr26)
2	20	21
1	22	23
0	03	14

Element nr 19 was replaced for a test, not because of malfunctioning.

Calibration and electronics of Pt500 elements

The calibration curve of a Platinum 500Ω element can be described within 0.01 Kelvin by the quadratic function:

$$T = 0.5118 \cdot (R-500) + 3.9 \cdot 10^{-5} \cdot (R-500)^2 \quad (4)$$

In the temperature range ±25°C R-500 varies between ±50Ω. The second order term then varies between ±0.1 Kelvin. If we want to measure to an accuracy of 0.1 K, the system has to reproduce the first order coefficient within 0.0010 and the second order coefficient within $2 \cdot 10^{-5}$.

The resistance bridges are compensated for the slight non-linearity in the calibration curve of the Platinum elements. The second order coefficient was found to be correct within 10 % which introduces a negligible error of < 0.01 K.

The Pt500 elements are used to arrive at absolute temperatures in the profiles. They are calibrated at the calibration laboratory of the KNMI against a reference temperature. The calibration curves did show deviations from the gauge Pt500 over the range -10 to +35 °C of 0.04Ω at most, corresponding to 0.02 Kelvin. Apart from this an overall offset was found corresponding to:

LEVEL 0 Tref = T(Pt500) + 0.03 K
LEVEL 1 Tref = T(Pt500) - 0.04 K

The resistance bridges were tuned for 500 Ω at 0° C in March 1988. In January 1990 the bridges were re-calibrated. Offsets were found in both bridges. In terms of simulated temperatures the offsets are:

LEVEL 0 T(sym) = T(out) - 0.10 K
LEVEL 1 T(sym) = T(out) - 0.08 K

where:

T(sym) is the simulated temperature (tolerance 0.01% ≡ 0.025K)
T(out) is the reading of the electronic circuit

To arrive at a correction we assume that the PT500 elements have not changed and the electronic offset has a constant drift in time. Averaged over the whole period we then have:

LEVEL 0 T(cor) = T(mes) - 0.02
LEVEL 1 T(cor) = T(mes) - 0.08

The estimated accuracy of the corrected values is 0.1 K.

At 29 august 1988 the dry-bulb sensor at level 1 was calibrated during 10 minutes in a water bath against a reference Pt500 sensor (accuracy 0.01K). The result was:

T(ref) = 16.60°C
T(mes) = 16.87°C

Taking into account the offsets just derived T(mes) should be corrected with -0.08K to 16.79 C with still a deviation of 0.19 K. This contradicts the claim just made. We must conclude that the accuracy of the absolute temperature measurements is not better then 0.2 K.

Calibration and accuracy of thermo-couples

For this project new thermocouple elements were produced at the KNMI. Each element consists of two junctions. A first series of 15 elements, KNMI NR 01-02-080-01 till 15, was produced with too short wires. They were only suitable for use at level 0. A second series of 11 elements was made, KNMI NR 01-02-080-16 till 25, which were used at the above forest levels. All the thermocouple junctions were made of one sample of Copper and Constantane wire.

For calibration a reference junction was kept at 0°C while the other junctions were varied over the temperature range of -20 to 40°C. For all junctions a third order regression was made. Except for some junctions of the first series the standard deviation of the residuals was only slightly larger then the assumed accuracy in the calibration system. An overall regression was made. Comparison of the standard error of estimate of this regression with those of the individual regressions revealed that there was no significant difference between the individual junctions. Consequently the overall regression can be applied to all the elements.

The second and third order polynomial fits and the standard error of estimate in T are given by:

$$T = 0.003 + 26.111 \cdot U - 0.819 \cdot U^2 + 0.071 \cdot U^3, \quad \sigma_T = 0.006 \qquad (5)$$

$$T = -0.024 + 26.148 \cdot U - 0.728 \cdot U^2 \quad , \quad \sigma_T = 0.024 \tag{6}$$

Where:
T Temperature of the calibrated junction in ^{0}C.
U Voltage relative to the junction at 0^{0}C in mV.

From this it is clear that the second order fit is accurate enough to be used for absolute temperature measurements.The inverse regressions are given by:

$$U = -0.095 + 38.309 \cdot T + 0.0458 \cdot T^2 + 6.0\ 10^{-5} \cdot T^3, \ \sigma_U = 0.25 \tag{7}$$

$$U = 0.328 + 38.280 \cdot T + 0.0437 \cdot T^2 \quad , \ \sigma_U = 0.46 \tag{8}$$

here U is in μV.

For small temperature differences (< 2 Kelvin) a linear calibration factor F_{tcop} with an accuracy better then 1% can be derived from the second order regression eq(8):

$$F_{tcop} = \frac{dU}{dT} = 38.28 + 0.0874 \cdot T_m \ (\mu V/K) \tag{9}$$

Where:
T_m Averaged temperature of the two junction in °C.

For small temperature differences (ΔT) this factor is accurate within 0.6% over the whole calibration range. For ΔT < 2.5 Kelvin the accuracy is better then 1%. For the same accuracy of 1%, T_m has to be known within 5 Kelvin.

Since the difference in temperatures in the profile seldom exceeds 2 Kelvin F_{tcop} can be used for these differences provided that T_m is chosen as a wet-bulb temperature in the wet-bulb profile and correspondingly a dry-bulb temperature is chosen in the dry-bulb profile. Since the temperature difference between wet-bulb and the dry bulb or the reference junction at the PT500 element can be as large as 13 Kelvin the non-linearized calibration curve should be used. Here the second order regression eq.(6) is appropriate.

The above forest temperature thermocouple system could be checked for internal consistency. Summing all the thermo-couple temperature differences (DELT) should add to zero. This sum does not give a check whether temperature sensors suffer from, for example, radiation effects or a dry wet-bulb sensor. It checks whether there are other effects than the usual sensor temperature differences that add to the thermocouple voltages. For example zero drift of amplifiers or chemical potentials in the thermo-couple system.

Electronics of Thermo-couples

From a first analysis it was shown that DELT varied linearly with the wet bulb depression. This effect can arise when amplification factors deviate from the specification. The amplification factors of the whole electronic system were determined with high precision.

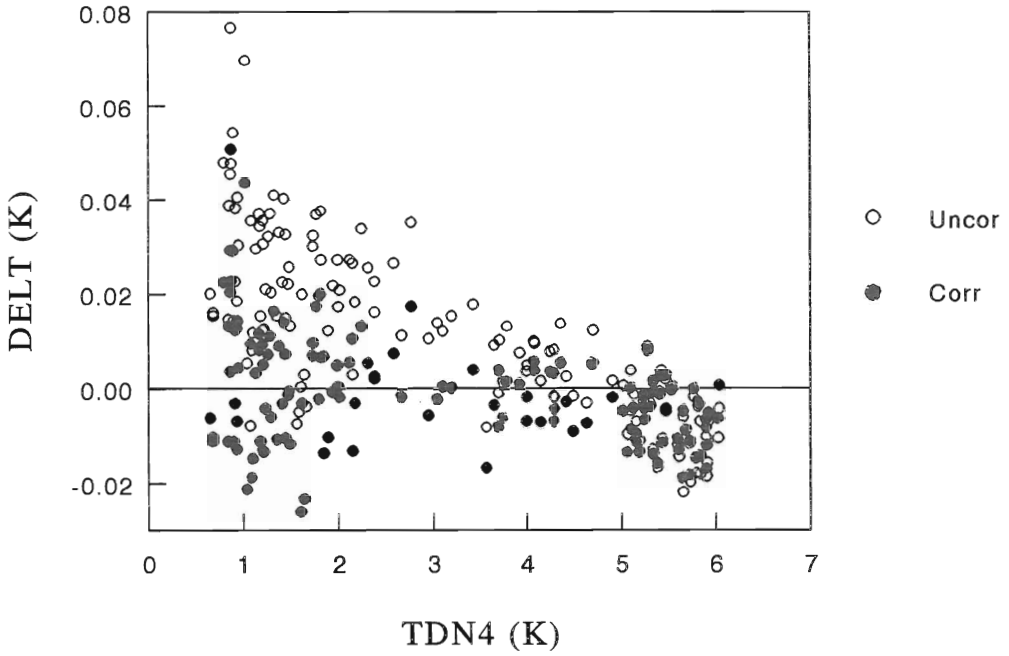

Figure 9 Residual temperature (DELT) of the thermo-couple system as a function of the wet-bulb depression at level 4 (TDN4) before and after correction.

Table 8 gives the resulting correction factors. Figure 9 gives DELT for one day as a function of TDN4 both before and after correction.

Particularly important are the possible offsets in the thermo-couple system. We are interested in an accuracy of about 0.02 Kelvin in the temperature differences. Zero-drifts in amplifiers and thermo-couple potentials introduced by temperature differences over inhomogeneities in the sensor cables or chemical potentials at contact points could well destroy this desired accuracy. From test-measurements with the sensors substituted by short circuits in the mast it was found that the cables themselves possibly introduce a variation of 0.02 Kelvin over the days. No diurnal rhythm was observed.

To obtain corrections for the offsets, measurements which met stringent criteria for atmospheric neutrality were analyzed. On the basis of 30 minute mean data theoretical temperature differences were derived from sensible heat flux eddy correlation measurements. If the theoretical difference was less then 0.05 Kelvin in absolute sense then the value was retained. If there were more than 4 half hour values retained in one day then this day was retained. From these values the average differences between theoretical- and experimental values were determined. Figure 10 shows the values throughout the year for TD21, TD43 and TD43. From this it can be seen that the offsets are fairly constant throughout the year.

For the estimation of wet-bulb temperature differences one needs to know the available

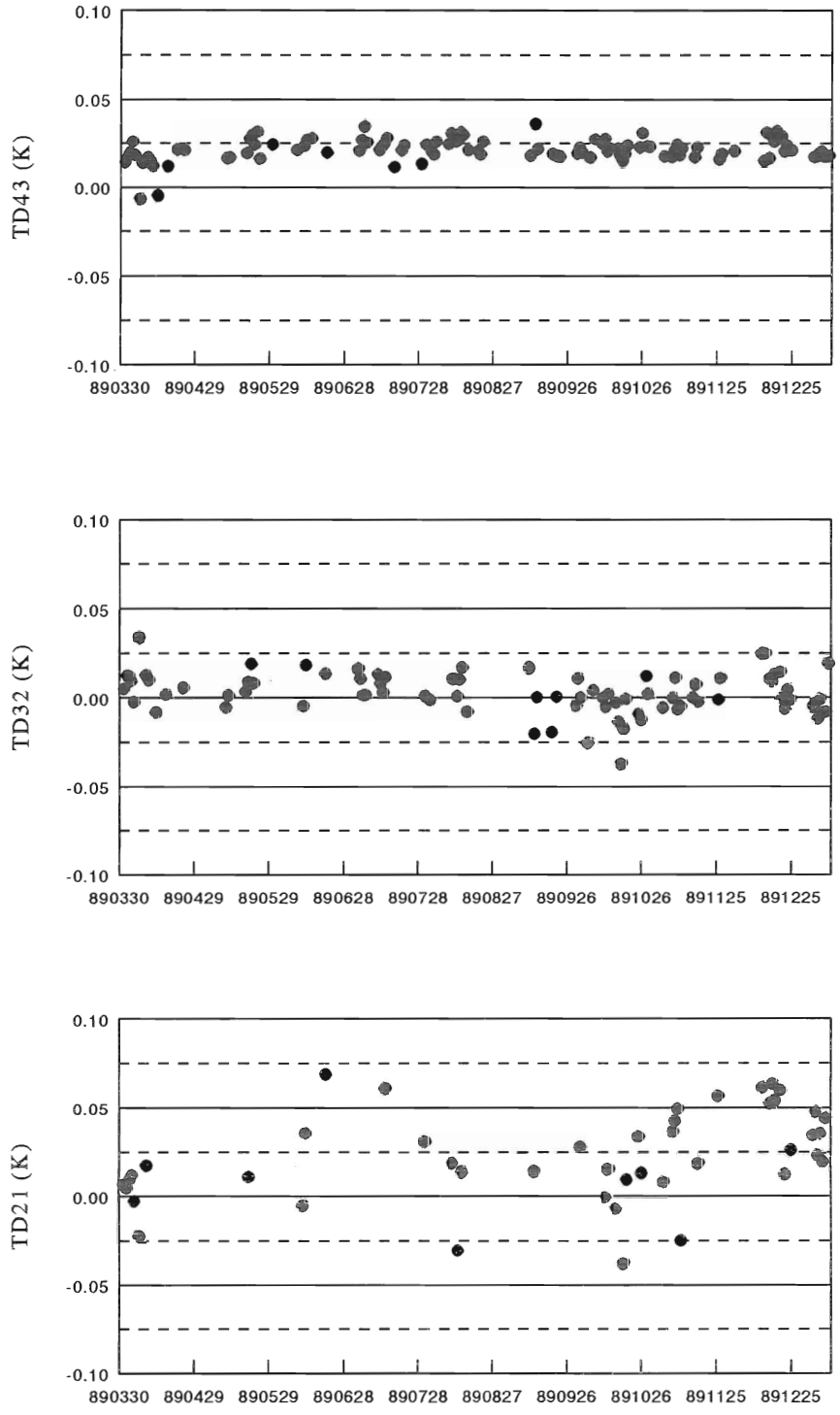

Figure 10 Difference between observed dry-bulb temperature difference between the successive levels and estimated values from eddy-correlation measurements for selected neutral conditions throughout the year.

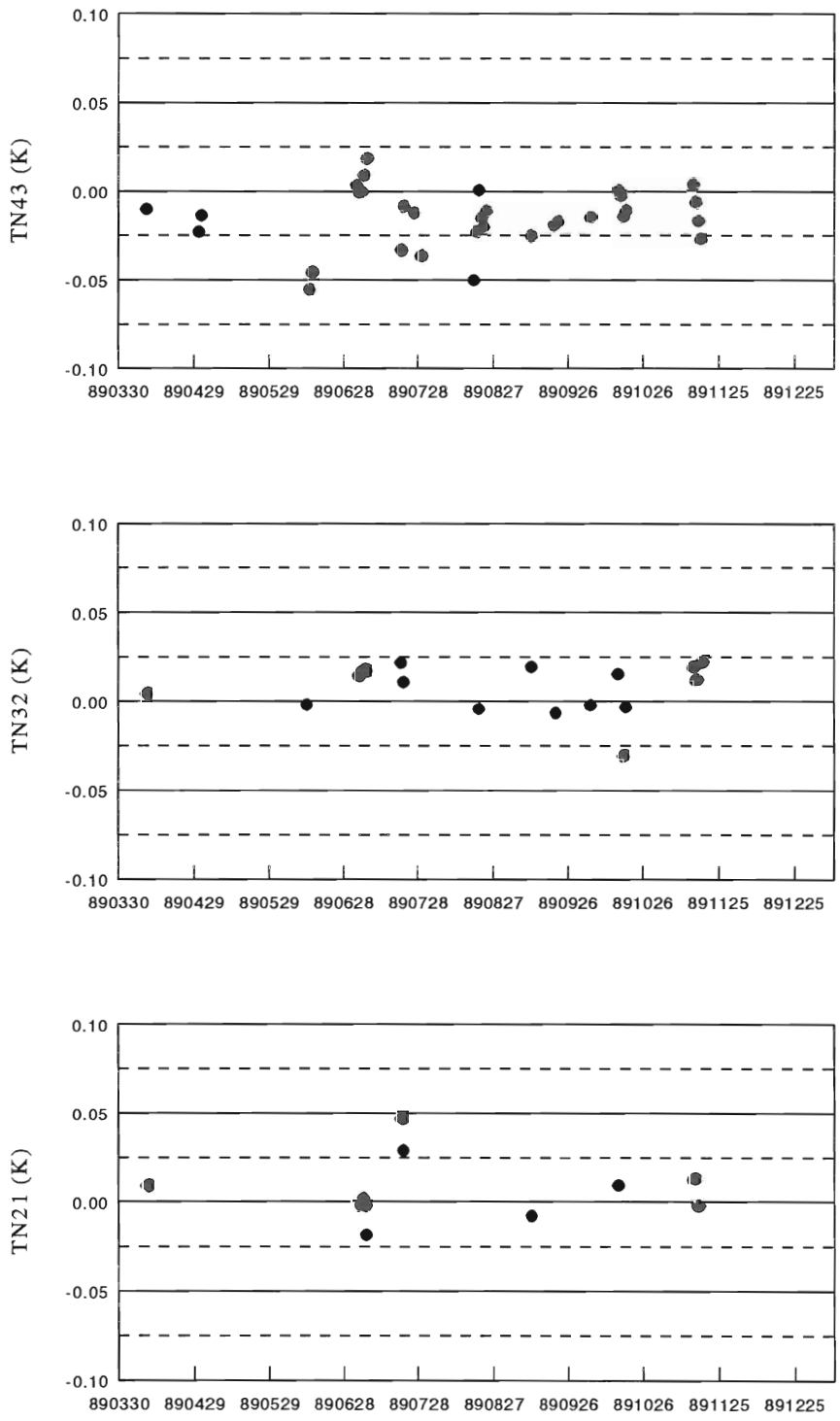

Figure 11 Difference between observed wet-bulb temperature difference between the successive levels and estimated values for small total heat flux derived from eddy-correlation measurements throughout the year.

heat flux. Since this involves eddy-correlation measurements of latent heat, considerably less days were found for which offsets could be estimated. Figure 11 shows the result. From this graphs correction offsets were estimated. Table 8 lists the offset corrections performed on the data-set.

4.2 Sonic thermometer

Instrument specification

Sonic temperature is measured with a Kaijo Denki DAT-300 sonic anemometer-thermometer system (Model TR-61A probe). The temperature measurements of the sonic anemometer are based on the determination of the velocity of sound (C) along the vertical path. Each 53 msec a measurement along the vertical path is taken which is converted to an analogous signal by an 11 bits D/A converter.

Calibration and accuracy

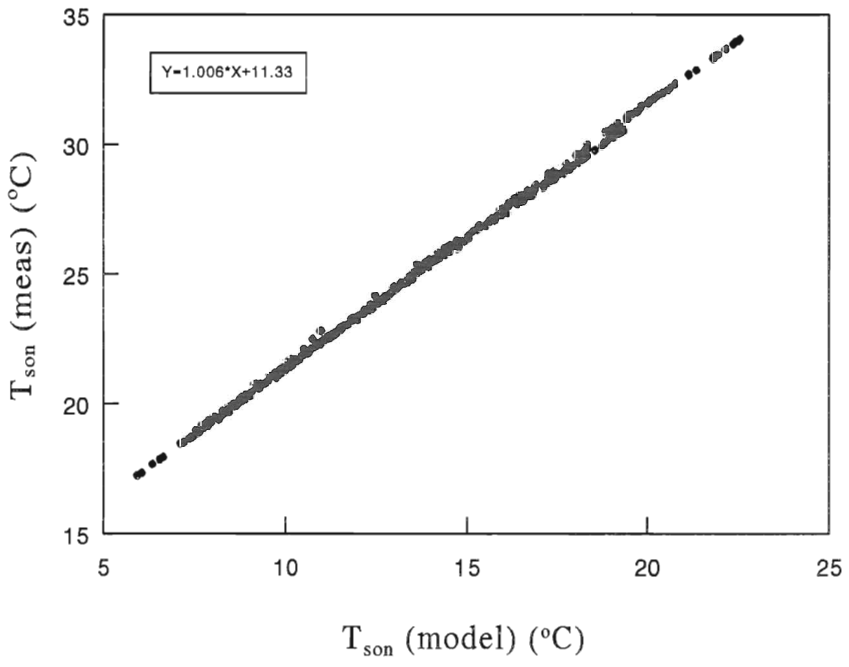

Figure 12 Comparison between measured sonic temperature and derived sonic temperature from dry-bulb, wet bulb and wind measurements.

Table 8 Offset and amplification corrections performed on the thermocouple measurements.

Couple	offset cor.	Factor cor.
TD21	+0.023	1.0010
TD32	+0.003	1.0027
TD43	+0.022	1.0000
TN21	-0.005	1.0015
TN32	+0.018	1.0007
TN43	+0.007	1.0012
TDN4	0	1.0028
TD1B	0	0.9995
TN1B	0	0.9990
TD0B	0	1.0010
TN0B	0	1.0010

The speed of sound depends on temperature and on the molecular weight of air which varies most notably through the variation of the moisture content. Also the sonic temperature signal is contaminated by the horizontal wind speed which enhances the length of the path over which the sound signal travels. According to Schotanus et al. (1982) the sonic temperature T_s can be written:

$$T_s = T \cdot (1 + 0.51q) - \frac{U_n^2}{401} \qquad (10)$$

where q is specific humidity (in kg/kg) and U_n is the horizontal wind speed. For the calibration of the sonical temperature we compared in-situ measurements of sonic temperature at 30m with modelled sonic temperature from dry bulb and wet bulb temperature and wind speed at 24m and 31m above the forest floor according to eq.(10). Figure 12 shows a scatter diagram of the result. A regression analysis shows that the sonic temperature deviate by less then 1 percent. No correction is applied for this deviation. The offset is electronically induced and has no influence on the fluctuations.

In figure 13 the difference between Sonic temperature and dry-bulb temperature is shown for a number of periods in 1989. The offset obtained from the previous analysis is applied to the sonic temperature data. Drawn are the measured difference and the theoretical difference according to eq.(10). It is observed that the measurements follow the prediction reasonable, however deviation of several tenth of degrees occur occasionally. The reason for the deviation is unknown. A possibility might be that hygroscopic dust on the transducers can give rise to slight deviations in the acoustic path length.

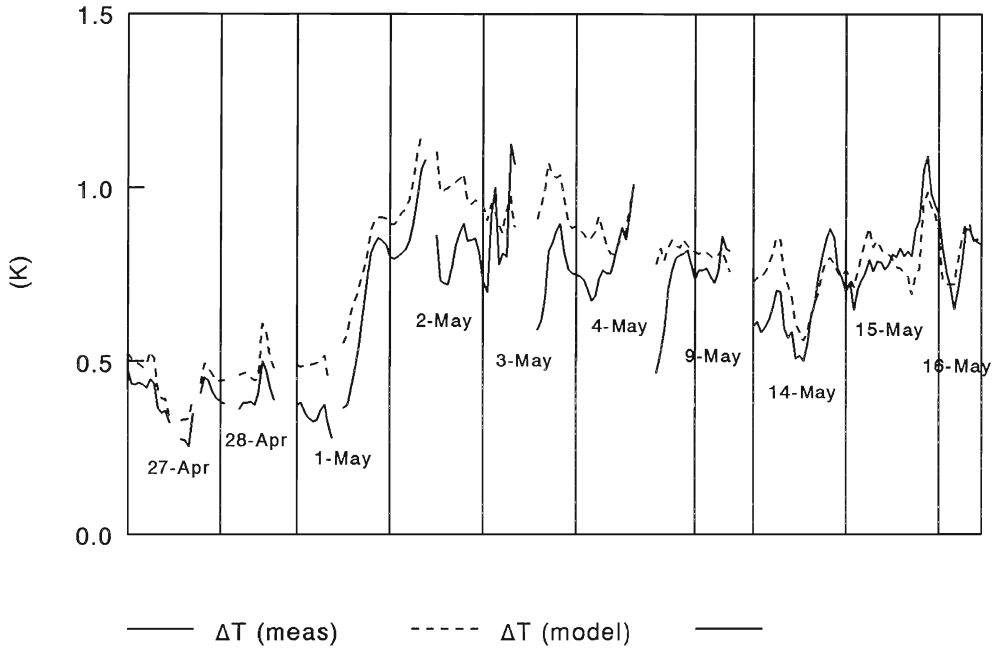

Figure 13 Moisture and wind effect on the sonic temperature. Measured and expected difference between measured sonic temperature and dry-bulb temperature.

Corrections on sonic temperature measurements.

To use the sonic temperature T_s for the determination of eddy-correlation temperature flux, corrections have to be applied for the humidity and wind effects. Schotanus et al. (1983) give a detailed derivation from which we take the correction equation for the temperature flux:

$$\langle ws \rangle = \langle wt \rangle + 0.51\ 10^{-3}\ \bar{T} \langle wq \rangle - 2\ \frac{\bar{T}\ \bar{U}}{C^2} \langle u_n w \rangle \qquad (11)$$

where <ws> the sonic temperature flux, <wt> is the temperature flux, <wq> the specific humidity flux, U the horizontal wind speed and $\langle u_n w \rangle$ the covariance between the fluctuation in the absolute horizontal wind speed and the fluctuation in the vertical wind speed. It is normal practice (Schotanus et al, 1982) to approximate $\langle u_n w \rangle$ by the kinematic stress along the averaged horizontal wind vector <uw> by neglecting higher order correlations in the wind fluctuation. To be precise we have to third order in the fluctuations of the wind:

$$2\bar{U} \langle u_n w \rangle = 2\bar{U} \langle uw \rangle + \langle u^2 w \rangle + \langle v^2 w \rangle \qquad (12)$$

Since wind fluctuations are large over the forest it remains to be shown that this approximation is correct for our situation. Six 10 minute time series of 5 Hz data were

analyzed and it was found that the sum of the two triple products amounts to 20% of the first term on the right hand side of eq.(12).

To estimate the importance of the correction we write equation (11) in terms of heat fluxes:

$$H_s = H + \frac{0.06}{\beta} H - 6.2\ \bar{U} \langle u_n w \rangle \qquad (13)$$

where β is the Bowen ratio which is typically 1 for the forest. This results in a moisture correction of about 6 %. For extreme wind conditions (U=10 m/s and <uw>=1.5 $(m/s)^2$ we have 90 W/m^2 and then the triple correlations can become important in the correction. However, for typical conditions (U= 4 m/s and <uw>=0.5 $(m/s)^2$) the wind correction is about 10 W/m^2 and thus the triple correlations are circa 2 W/m^2, which is well below the assumed accuracy for this kind of measurements. Consequently, no triple product corrections are performed.

If only the wind correction is applied to the sonic temperature flux we end up with a quantity which is almost equal to the virtual temperature flux which is given by:

$$\langle wt \rangle (virtual) = \langle wt \rangle + 0.61 10^{-3} \langle wq \rangle \qquad (14)$$

which is proportional to the buoyancy flux. This quantity then can be used in the calculation of the Obhukov length scale.

Wind corrections can be performed on the basis of sonic wind measurements. The moisture flux correction is more difficult. In periods that humidity fluctuation measurements are present corrections can be performed on the basis of these flux determinations. Specific humidity profile measurements were found to be too unreliable to derive moisture fluxes from. It was decided to base the correction on the Single Big Leaf model transpiration as described by Bosveld et al.(1993). This model gives the transpiration of the forest on an hourly basis with an accuracy of 30 W/m^2, accurate enough for our purpose. For periods when the canopy is wet during and after rain events this method cannot be used since part of the latent heat flux then originates from the evaporation of the free liquid water at the canopy which is not accounted for in the model. During such periods the sonic temperature measurements are less reliable anyway since liquid water on the transducers distorts the transmission of the sound pulses.

4.3 Pt-cold wire thermometer

During a limited period temperature fluctuations were measured with a Platinum cold-wire device. It is used as a direct check for deriving temperature fluxes from the sonic temperature sensor, and because of its high time resolution it is used to measure structure parameters of temperature. For a description of the instrument and its calibration procedure see Kohsiek (1987).

Instrument specification

Resistance	50 Ohm
Thickness	2.5 μm
Length	3 mm

High frequency cut-off 700 Hz

Corrections

A correction factor of 1.03 was applied to the temperature fluctuation data as suggested by Kohsiek (1987,p4). This correction is due to a discrepancy between the actual temperature coefficient of the Platinum wires and the one used in the resistance bridge.

4.4 Ly-α Hygrometer

The Ly-α hygrometer measurements are based on the extinction of the Ly-α 121.56nm ultra-violet hydrogen line over a path of a few centimetres. The advantage of using this Ly-α line is that the oxygen spectrum shows a dip in its extinction just at this wavelength. Would this not be the case a quite large temperature cross-talk signal would show up due to the fluctuation of oxygen density with temperature. In practice the UV-light source is not monochromatic, resulting in an extinction different from the ideal Beers-law. For details see Buck (1978).

Instrument specification

Manufacturer:	Electromagnetic Research Corporation
Source:	Glass Technology, Magnesium Fluoride optics, diameter 0.9 cm.
Detector:	Glass Technology
Path length:	0-3 cm

The response is limited by the path averaging and not by the sensor or electronic response times. For a path of 1 cm and a wind speed of 3 m/s the characteristic time of response is 3 ms.

Electronics: The detector current is amplified and fed into a logarithmic amplifier

Calibration and accuracy

The calibration procedure and the implementation of the calibration in the field is described by Kohsiek (1986). During the two years of operation several Ly-α tubes were used. The calibration dates and operation periods are listed in table 9. Source number GT11 was re-calibrated in october 1989. The two calibration curves showed significant differences. To decide which curve was the right one the field measurements were used to derive a third curve. Periods were selected where the Ly-α signal showed a stable behaviour. Due to transmission changes of the optics considerable shift on the Ly-α signal can occur. For each consecutive period with a stable Ly-α signal a point of the calibration curve was derived. Figure 14 shows the results of each period in a calibration diagram. Displayed are also the April and October calibrations together with an on eye fitt through

Table 9 Ly-α tubes, calibration date and period of operation.

Source number	Calibration date	Period of operation
GT 4	Mar 1988	26/04 - 12/05 1988
GT 8	Aug 1988	01/09 - 01/10 1988
GT10	Mar 1989	30/03 - 01/04 1989
GT11	Apr 1989	08/04 - 19/10 1989
GT12	Nov 1989	13/11 - 10/01 1990

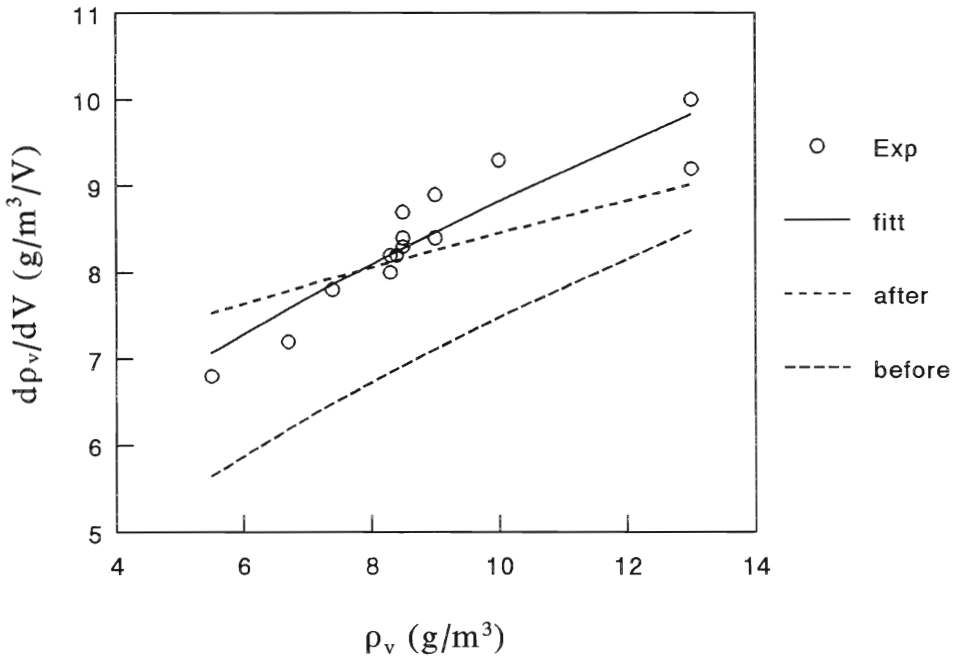

Figure 14 Sensitivity of Ly-α with source GT11. Pre-calibration, post-calibration and field values.

the field-data. From this analysis it is clear that the calibration of October 1989 most closely approaches the on-situ derived calibration. Decided was to use the October calibration curve and correct the original data accordingly.

Operation and maintenance

Previous optics of Lithium Florid could easily be etched by water. The present optics with Magnesium Fluoride is less sensitive to water. Despite this improvement very thin layers of water already extincts the UV-light completely and thus after a rain episode the apparatus doesn't function for quite a long time. Moreover the evaporated rain water

leaves behind thin layers of dust which also decrease the transmission considerably. The Ly-α hygrometer was only operated during special observation periods. At each installation the detector and source where tested for stability and dark-current. Also the optics was cleaned with alcohol.

Corrections

The Ly-α measures the water vapour density fluctuations. Even in the absence of water vapour fluctuations the presence of temperature fluctuations induce an water vapour density fluctuation. Webb et al. (1980) describes the resulting correction. This correction is performed on the data.

5 Radiation

5.1 Global radiation

Instrument specification

Total shortwave incoming radiation was measured with a Kipp pyranometer type CM 11, KNMI nr 01.23.010.42. The thermocouple signal from the thermopile was amplified by a R&H amplifier. The output current was led through a 250 Ω resistor, resulting in an amplification of 500 times. The amplifier was checked at the beginning and the end of the measuring campaign and showed a deviation of less then 1 ‰.

Calibration and accuracy

The instrument was calibrated at the KNMI in April 1987. The sensitivity was 4.84 $\mu V/(W/m^2)$.

Operation and maintenance

Domes were cleaned each week with de-mineralized water. Levelling was checked on a regular basis.

5.2 Net radiation

Instrument specification

Net radiation was measured with a Funk net-radiation meter. Both sides of the instrument were covered with poly-ethylene domes which were kept under pressure by dry Nitrogen. The instrument was ventilated till July to avoid dew formation.

Electronically an offset of 8mV was added to the incoming signal which corresponds to approximately 180 W/m^2 . This was necessary since the R&H amplifier was only capable of amplifying positive voltages. The amplification factor was 62.11. Over the total period this factor was stable within 0.5%. The offset was stable within some tenths of a W/m^2.

Operation and maintenance

Domes were replaced approximately each month. In June and July of 1989 the domes were picked frequently by birds. At the 17th of July the instrument was replaced by a new one since the blackening of the sensor surface had suffered too much from these attacks. To prevent birds from having a comfortable rest place the ventilation was dismantled.

Calibration and accuracy

Calibration for short-wave radiation was performed at the KNMI. The results are tabulated in table 10 together with periods of operation. Compared with earlier calibrations performed throughout the last decennium, variations were smaller then 1% although the blackening of instrument nr 01 was not optimal at the last calibration. Calibration for long-wave radiation has been performed at the KNMI in 1976. These calibrations indicate a deviation of the long-wave sensitivity of less then 1% compared to the short-wave sensitivity. In the original data-set a sensitivity of 44.55μV/(W/m^2) is assumed. In the final data-set the values are corrected with the new calibration values.

The largest uncertainty arises from the degradation of the poly-ethylene domes. A comparison of the sensitivity for short-wave radiation with old domes (more then one month in operation) and new domes showed a higher sensitivity of 4% for the new domes. This last number is then an indication of the overall accuracy of the instrument.

Tilted net radiation sensor

During the experiment doubt raised whether the net radiation meter was properly placed horizontally. The sensor was mounted on a 3 m long boom that could be rotated along the mast side for maintenance. The sensor was always placed horizontal when the boom was rotated along the mast. However, the axis of boom rotation appeared to be not entirely vertical. A closer inspection suggested that the sensor was tilted a few degrees to the south along the boom axis which points in the direction 120° relative to north.

From an analysis of the radiation balance for clear days in 1989 it was derived that the tilting angle should be 4.5 degrees. The main error results from direct sunlight. With an algorithm for deriving direct sunlight from measured global radiation a correction procedure for this tilting was derived.

5.3 Radiation Temperature

Instrument specifications

Infrared radiation temperature is measured with a Heimann infrared thermometer Type KT-24. The instrument is sensitive in the spectral range 8-35μm. The instrument is mounted at the 36 m level and looks at the forest crowns at azimuth 350° with an

Table 10 Funk net radiation instruments, calibration and period of operation.

KNMI Nr	Calibration date	Period of operation	Calibration factor
01.23.030-01	Apr 1990	26/4/88-17/7/89	44.28 (μV/Wm^2)
01.23.030-03	Apr 1990	18/7/89-13/1/90	42.94

elevation of -45°. The instruments optics has an half-opening angle of 22°.

To avoid temperature gradients inside the sensor the instrument is kept at constant temperature by means of a thermostat. From 6 May 1988 on the thermostat temperature was at 30°C. At 6 and 7 July 1989 air temperatures were above 30°C and consequently the temperature of the Heimann rose up to 33.8°C at 6 July and to 30.9°C at 7 July.

Calibration and accuracy

Calibration was performed at the KNMI in 1987 against a water bath at thermostat temperatures of 20°C and 40°C. A preliminary analysis showed that the laboratory calibration for 40°C did show systematic differences over the relevant temperature range of ±1 Kelvin. The 20°C calibration did show larger deviations. Probably the different thermostat temperature is to blame.

6 Other Instruments and indicators

6.1 Scintillometer

During fall 1988 and spring 1989 a near infrared scintillometer was operated. The source was located at a tower in Drie, 1.5 km North of the research location. The receiver was in the top of the KNMI mast. The instrument measures the scintillation of the index of refraction in the air due to density fluctuations introduced by temperature and humidity fluctuations. Effectively it gives a structure parameter averaged over the 1.5 km long optical path. For details on the instrument see Kohsiek (1987). Results are presented in Kohsiek (1992).

6.2 Rain indicator

An ECN-type rain indicator was operated during the measuring period at 36m height. The sensor consists of four isolated plates placed in a pyramidal shape. Each plate elevated at an angle of circa 30^{o}. The plates hold two patterns of copper traces which are short circuited when water is present on the sensor. A heating current serves to dry the sensor. after the rain has stopped. The sensor produces a simple on (+4.3 Volt) and off (0 Volt) signal.

6.3 Pressure

Air pressure was registrated with a Fuess Barograph. The instruments performed one cycle a week. At the beginning and the end of the registration the barograph was referenced wit precision aneroid barometer (Negretti & Zambra). A height correction of 6.5 hPa was applied to arrive at mean sea level pressure. Registrations were stored at KNMI.

6.4 A/D offset

During 1988 there were problems that even a short circuited A/D channel showed an offset of several mVolts. The problem seemed to be connected with current through ground. Although the problem was partly remedied before 1989, a small offset remained during the 1989 measuring period. To diagnose this effect one channel was short circuited and registrated parallel with the other signals. No corrections were performed for this.

7 Database

Data are sampled and reduced on-line to 10 minute values. These basic quantities are fed into a database. The database consists of day-files. These are FORTRAN REAL*4 (IEEE floating point format) unformatted direct access files. The 10 minute data coming from the field are gathered into day-files called SP<day>.A10, where <day> is in the format YYMMDD (thus the 8th of june 1989 reads 890608). These day-files have 300 columns and 144 rows.

A second database is created which is a copy of the first one but in which unreliable data are removed, corrections are performed and new quantities are derived from the basic data. Standard is a 30 minute database, file names SP<day>.B30, but databases with other time intervals can be generated as well.

Appendix A tabulates the contents of the columns of the day-files

7.1 On-line calculation of the basic quantities

At the site 34 signals are sampled at a rate of approximately 1 Hz. On-line 10 minute values are calculated and stored on disk. These are:

- End time of the 10 minute interval
- Number of samples taken (N)
- Average value of each signal S according to:

$$<S> = \frac{1}{N} \cdot \sum_{i=1}^{N} S_i \qquad (15)$$

- Standard deviation of each signal S according to:

$$\sigma_S = \sqrt{\frac{1}{N} \cdot \sum_{i=1}^{N} (S_i - S_1)^2 - (<S> - S_1)^2} \qquad (16)$$

- Covariances of all fast response signals Q,R according to:

$$<qr> = \frac{1}{N} \cdot \sum_{i=1}^{N} (Q_i - Q_1) \cdot (R_i - R_1) - (<Q> - Q_1) \cdot (<R> - R_1) \qquad (17)$$

- Structure parameters and cross-structure parameters of several fast response signals according to:

$$C_{QR}=\frac{\frac{1}{N}\cdot\sum_{i=1}^{N}\left[Q(t_i+\tau)-Q(t_i)\right]\left[R(t_i+\tau)-R(t_i)\right]}{(U\tau)^{2/3}} \qquad (18)$$

where τ is the time interval and U is the average length of the horizontal wind vector estimated from the sonic anemometer measurements according to :

$$<|\vec{U}|>=|<\vec{U}>|+\frac{1}{2}\frac{<vv>}{|<\vec{U}>|} \qquad (19)$$

where <vv> is the variance of the lateral wind component.

- The calibration factor used for transforming Ly-α voltages to water vapour density. This factor is derived from a calibration curve and the measured water vapour density.

- The shift in the Ly-α voltage relative to the reference calibration, this gives an indication of the transmission drift of the optics.

- The azimuth of the rotator at the beginning and at the end of the 10 minute interval.

- The fraction of samples that the rain indicator indicates rain.

For the horizontal wind the A-sensor and B-sensor of the sonic anemometer system are sampled and transformed to an orthogonal coordinate system according to eq.(3). Consequently horizontal wind vector samples are relative to the sonic frame. If the rotator is turned during the 10 minute interval then the next horizontal wind vector samples are transformed to the coordinate system of the beginning of the interval. At the end of the measuring interval all covariances related to the horizontal wind components are transformed to the coordinate system along the average horizontal wind vector. See figure 6a for the definition of the coordinate system. All basic 10 minute average quantities are scaled to physical quantities according to a calibration table before writing them to disk.

7.2 Data screening

A first check on the data was performed on site. Hard copies of 10 minute averages were inspected to detect malfunctioning of the instruments and appropriate action could be taken. Approximately each week data were transported to KNMI. There relevant quantities were inspected through visualisation of time series in a spreadsheet (LOTUS 123). Suspect values were removed from the data-set and if necessary instruments were checked on the site. Information on which data had to be removed was kept in files SP<day>.CLN associated with the corresponding data-file SP<day>.A10 together with a brief description of the reason why the value was removed.

Frequently encountered reasons why data were removed are:

- Maintenance of the instruments.
- Dry wet-bulb sensors.
- Damaged domes of the net-radiation sensor.

During rain some instruments do not function properly. Most notably:

- Dry-bulb temperature becomes wet. Since the wet-bulb depression tends to be low during rainy conditions this situation is hard to detect. Data are not removed.
- Sonic temperature and to a lesser extend the sonic vertical wind speed signal becomes erratic because of water on the vertical transducer. Only when the deviations are clearly visible data are removed

Other instruments can show less obvious deviations during rain:

- Wet-bulb temperature becomes to low because of colder rain water on the sensor. Data are not removed.
- Impact of rain drops on the cup anemometers, likely to increase the rotation speed. Data are not removed.
- Drops on the domes of radiation sensors can, by refraction change the amount of intercepted radiation. Data are not removed.

During frost wet bulb temperatures were removed from the database.

Removing data from the database was performed by changing the value to -9999 indicating a missing value.

7.3 Corrections

From the analysis presented here and in Bosveld (1997) several corrections were obtained. They involve:

A) Corrections due to recalibration of instruments and electronics:

- Adjustment of calibration factors.
- Adjustment of offsets.

  In the data base the old values are replaced.

B) Corrections due to known physical reasons:

- Tilting of the net radiometer. (To be decribed elsewhere)
- Flow obstruction around the sonic anemometer, both elevation and azimuth. (To be decribed elsewhere)
- Corrections for the sensitivity of the sonic wind speed measurements to angle of

onflow. (Bosveld, 1997)
- Wind and moisture correction for the sonic temperature measurements. (Schotanus, 1983)
- Density correction to moisture fluctuation measurements (Webb et al., 1980).
- Overspeeding corrections on the cup anemometer measurements (Bosveld, 1997).
- Correction for response loss of the structure parameter of the vertical wind (Van der Ploeg, 1995 and Bosveld, 1997)

The corrected values are placed in new columns in the data file. This makes it possible to investigate the effect of the corrections. In a way these are derived quantities.

7.4 Derived quantities

Relevant quantities for future analysis were derived from the basic quantities and placed in new columns of the data-file. Before calculating this values the basic quantities on which the derived quantity depend are checked for missing value and if so the derived quantity was set to missing value as well.

7.5 On the sequence of calculations

The order in which corrections are applied, derived quantities are calculated and average values are derived is important. For example, before a quantity is used for deriving a dependent quantity or to correct a quantity, it has to be corrected itself. The following line is followed.

1) Calibration corrections on basic quantities are performed. If another basic quantity is needed for the correction this quantity has to be corrected first. No use is made of derived quantities.

2) Physical corrections are calculated which preferably should be performed on the 10 minute values. For example, the correction on the tilted net radiation meter which involves a scheme to estimate the direct solar radiation. This scheme gives the best result on short time intervals.

3) Quantities derived from a non-linear functions of basic quantities should preferably be calculated on a 10 minute basis and then averaged.

4) Appropriate averaging is performed over three or six 10 minute intervals.

5) Calculate those derived quantities that can safely be derived from the averaged basic quantities, this saves computing time.

6) Calculate those quantities that should be derived from averaged quantities due to turbulence statistics (e.g. fluxes from profiles and stability).

8 Acknowledgements

Designing, building and running a micro-meteorological mast is a large effort which involve many people. In the first place we like to thank M. P. D. Jansse of INSA for a perfect managing of the build up phase of the project. Mark van Wijngaard and Bob van de Berg for designing and drawing. Willem Hovius, Roel Blankestein and Sjaak Koster of INSA for actual build up work. Special thanks also for Rob van Krimpen of the calibration laboratory for careful and tedious calibration work on cup anemometer and temperature sensors. Dr. Wim Kohsiek for many advices. Last but not least we like to thank Dr. Adrie Jacobs and Anton Jansse of the Agricultural University of Wageningen for lending their cup anemometers.

9 Literature

Bosveld F.C., W. Bouten and F. Noppert, 1993. Transpiration dynamics of a Douglas fir forest II: parametrization with a single big leaf model. In: W. Bouten; Monitoring and modelling forest hydrological processes in support of acidification research. Thesis University of Amsterdam, The Netherlands.

Bosveld F. C. (1997). Derivation of fluxes from profiles over a moderately homogeneous forest. Boundary layer meteorology, 85, 289-326.

Buck A.L., 1976. The variable path lyman-alpha hygrometer and its operating characteristics. Bull. Am. Meteor. Soc., 57, 1100-1124.

Evers P.W.(ed), 1991. CORRELACI, Identification of traditional and air pollution related stress factors in a Douglas fir ecosystem: the aciforn stands. De Dorschkamp Report nr. 623. "De Dorschkamp" Research Institute for Forestry and Urban Ecology, Wageningen, The Netherlands.

Kohsiek W., 1985. A CO_2 laser scintillometer for C_N^2 measurements over a many kilometer path. KNMI Technical Report TR-67. Royal Netherlands Meteorological Institute, De Bilt, The Netherlands.

Kohsiek W., 1986. The KNMI Lyman-alpha hygrometer. KNMI Technical Report TR-87. Royal Netherlands Meteorological Institute, De Bilt, The Netherlands.

Kohsiek W., 1987. A device for measuring fast temperature fluctuations. KNMI Technical Report TR-92. Royal Netherlands Meteorological Institute, De Bilt, The Netherlands.

Kohsiek W., 1992. A Scintillation experiment over a forest. KNMI Scientific report WR 92-04. Royal Netherlands Meteorological Institute, De Bilt, The Netherlands.

Kraan R. and W.A. Oost, 1989. A new way of anemometer calibration and its application to a sonic anemometer. J. of Atmospheric and Oceanic Technology, 6, 516-524.

Kristensen L., 1993. The cup anemometer and other exciting instruments. Risø-R-615(EN), Risø National Laboratory, Roskilde, Denmark, April 1993.

Lumley and Panofski (1964). The structure of atmospheric turbulence. Wiley Interscience, New York.

Monna W. A. A., 1983. De KNMI windtunnel. KNMI Tecnical report TR-32. Royal Netherlands Meteorological Institute, De Bilt, The Netherlands. (In Dutch)

Schotanus P. (1982). Turbulente fluxen in inhomogene omstandigheden. KNMI scientific report WR 82-3. Royal Netherlands Meteorological Institute, De Bilt, The Netherlands. (In Dutch)

Schotanus P., F.T.M. Nieuwstadt, H.A.R. De Bruin, 1983. Temperature measurement with a sonic anemometer and its application to heat and moisture fluxes. Boundary layer meteorology, 26, 81-93.

Schneider T. and A.H.M. Bresser, 1986. Dutch priority programme on acidification; Report nr 00-01, programme and projects. RIVM, Bilthoven, The Netherlands.

Slob W.M., 1978. The accuracy of aspiration thermometers. KNMI scientific report 78-1. Royal Netherlands Meteorological Institute, De Bilt, The Netherlands.

Tiktak A. and W. Bouten, 1990. Soil hydrological system characterization of the two ACIFORN stands using monitoring data and the soil hydrological model "SWIF". Project nr. 102.2-01 of the Dutch Priority Programme on Acidification. Laboratory of Physical Geography and Soil Science, University of Amsterdam,The Netherlands.

Van der Ploeg R., 1995. Measurements of the structure parameter of the vertical wind-velocity in the atmospheric boundary layer. KNMI technical report 173. Royal Netherlands Meteorological Institute, De Bilt, The Netherlands.

Vermetten A.W.M., P. Hofschreuder and H. Harsema, 1986. Deposition of gaseous pollutants in a Douglas Fir forest. H.-W. Georgii (ed.) Atmospheric pollutants in forest area, 3-11. D.Reidel publishing company.

Webb E. K. , G. I. Pearman and R. Leuning (1980). Correction of flux measurements for density effects due to heat and water vapour transfer. Q. J. R. Meteorol. Soc. , 106, 85-100.

Wessels H.R.A., 1983. Distortion of the wind field by the Cabauw meteorological tower. KNMI scientific report 83-15. Royal Netherlands Meteorological Institute, De Bilt, The Netherlands.

Wylie R.G. and T. Lalas, 1981. The WMO reference psychrometer. Published by CSIRO, Australia, for distribution by the WMO.

A Column description

This appendix lists the contents of the database. The meaning of the basic quantities is in general straight forward and explained in chapter 7. The way other quantities are derived from the basic quantities can be found in the program listings below. The first column is a sequence number, the second the name identification, the third the physical unit, the fourth a code which indicates the way the quantity has to be averaged and the fifth gives a description of the quantity.

Column description of data base SPEULD

0	DAG	yymmdd	3	Time identification
1	BTIJD	hhmm	3	Begin time of interval (UTC)
2	ETIJD	hhmm	4	End time of interval (UTC)
3	DAGNR	-	3	Day number from beginning of the year
4	DLOTNR	-	3	Day number from 1 jan 1900
5	NSAMP	-	6	Number of samples
6	ROTR	o	1	Rotor azimuth
7	YSON	m/s	1	Windspeed sonic longitudinal component
8	XSON	m/s	1	Windspeed sonic lateral component
9	WSON	m/s	1	Windspeed sonic vertical component
10	TSON	K	1	Temperature sonic
11	PT50	K	1	CO2 Infrared open-path
12	LYAL	V	1	H2O Infrared open-path
13	TBL1	oC	1	Temperature PT-500 LEVEL 1
14	TD1B	K	1	Temperature difference LEVEL 1-PT500(1)
15	TD21	K	1	Temperature difference Dry LEVEL 2-1
16	TD32	K	1	Temperature difference Dry LEVEL 3-2
17	TD43	K	1	Temperature difference Dry LEVEL 4-3
18	TDN4	K	1	Temperature difference Dry-Wet LEVEL 4
19	TN43	K	1	Temperature difference Wet LEVEL 4-3
20	TN32	K	1	Temperature difference Wet LEVEL 3-2
21	TN21	K	1	Temperature difference Wet LEVEL 2-1
22	TN1B	K	1	Temperature difference Wet LEVEL 1-PT500(1)
23	TBL0	oC	1	Temperature PT500 LEVEL 0
24	TD0B	K	1	Temperature difference Dry LEVEL 0-PT500(0)
25	TN0B	K	1	Temperature difference Wet LEVEL 0-PT500(0)
26	UCUP0	m/s	1	Wind speed LEVEL 0
27	UCUP1	m/s	1	Wind speed LEVEL 1
28	UCUP2	m/s	1	Wind speed LEVEL 2
29	UCUP3	m/s	1	Wind speed LEVEL 3
30	UCUP4	m/s	1	Wind speed LEVEL 4
31	DDVN4	o	5	Wind direction LEVEL 4
32	GLOB	W/m2	1	Short wave downward radiation
33	QNET	W/m2	1	Net radiation
34	HEIM	V	1	Heiman infrared sensor (Voltage)
35	SCIN	V	1	Scintillometer (Voltage)
36	RAIN	V	1	Rain indicator
37	YWAT	o	1	Y-Inclinometer
38	XWAT	o	1	X-Inclinometer
39	OFFS	mV	1	Offset voltage of short-circuit A/D-channel
40	DCO2	ppm	1	CO2 concentration difference between LEVEL 4 and 2
41	SROTR	o	1	Sdv. Rotor azimuth
42	SYSON	m/s	1	Sdv. Windspeed sonic longitudinal component
43	SXSON	m/s	1	Sdv. Windspeed sonic lateral component
44	SWSON	m/s	1	Sdv. Windspeed sonic vertical component
45	STSON	K	1	Sdv. Temperature sonic
46	SPT50	K	1	Sdv. CO2 Infrared open-path
47	SLYAL	V	1	Sdv. H2O Infrared open-path
48	STBL1	oC	1	Sdv. Temperature PT-500 LEVEL 1
49	STD1B	K	1	Sdv. Temperature difference LEVEL 1-PT500(1)
50	STD21	K	1	Sdv. Temperature difference Dry LEVEL 2-1
51	STD32	K	1	Sdv. Temperature difference Dry LEVEL 3-2
52	STD43	K	1	Sdv. Temperature difference Dry LEVEL 4-3
53	STDN4	K	1	Sdv. Temperature difference Dry-Wet LEVEL 4
54	STN43	K	1	Sdv. Temperature difference Wet LEVEL 4-3
55	STN32	K	1	Sdv. Temperature difference Wet LEVEL 3-2
56	STN21	K	1	Sdv. Temperature difference Wet LEVEL 2-1
57	STN1B	K	1	Sdv. Temperature difference Wet LEVEL 1-PT500(1)
58	STBL0	oC	1	Sdv. Temperature PT500 LEVEL 0

59	STD0B	K	1	Sdv. Temperature difference Dry LEVEL 0-PT500(0)
60	STN0B	K	1	Sdv. Temperature difference Wet LEVEL 0-PT500(0)
61	SUCUP0	m/s	1	Sdv. Wind speed LEVEL 0
62	SUCUP1	m/s	1	Sdv. Wind speed LEVEL 1
63	SUCUP2	m/s	1	Sdv. Wind speed LEVEL 2
64	SUCUP3	m/s	1	Sdv. Wind speed LEVEL 3
65	SUCUP4	m/s	1	Sdv. Wind speed LEVEL 4
66	SDDVN4	o	1	Sdv. Wind direction LEVEL 4
67	SGLOB	W/m2	1	Sdv. Short wave downward radiation
68	SQNET	W/m2	1	Sdv. Net radiation
69	SHEIM	V	1	Sdv. Heiman infrared sensor (Voltage)
70	SSCIN	V	1	Sdv. Scintillometer (Voltage)
71	SRAIN	V	1	Sdv. Rain indicator
72	SYWAT	o	1	Sdv. Y-Inclinometer
73	SXWAT	o	1	Sdv. X-Inclinometer
74	SOFFS	mV	1	Sdv. Offset voltage of short-circuit A/D-channel
75	SDCO2	ppm	1	Sdv. CO2 concentration difference between LEVEL 4 and 2
76	UU	(m/s)2	1	Variance longitudinal wind
77	UV	(m/s)2	1	Covariance longitudinal- en lateral wind
78	UW	(m/s)2	1	Stress
79	US	Km/s	1	Covariance longitudinal wind en temperature SONIC
80	UT	Km/s	1	Covariance longitudinal wind en temperature PT50
81	UQ	gm/Kgs	1	Covariance longitudinal wind en specific moisture
82	VV	(m/s)2	1	Variance lateral wind
83	VW	(m/s)2	1	lateral stress
84	VS	km/s	1	Covariance lateral wind en temperature SONIC
85	VT	Km/s	1	Covariance lateral wind en temperature PT50
86	VQ	gm/Kgs	1	Covariance lateral wind en specific moisture
87	WW	(m/s)2	1	Variance vertical wind
88	WS	km/s	1	Temperature flux SONIC
89	WT	Km/s	1	Temperature flux PT50
90	WQ	gm/Kgs	1	specific moisture flux
91	SS	K2	1	Variance temperature SONIC
92	ST	K2	1	Covariance SONIC and PT50 temperature
93	SQ	gK/Kg	1	Covariance specific moisture en temperature SONIC
94	TT	K2	1	Variance temperature SONIC
95	TQ	gK/Kg	1	Covariance specific moisture en temperature PT50
96	QQ	g2/Kg2	1	Variance specific moisture
97	CAA1	-	1	Structure parameter ASON T=0.08 s
98	CAA2	-	1	Structure parameter ASON T=0.16 s
99	CAA4	-	1	Structure parameter ASON T=0.32 s
100	CAB1	-	1	CROSS Structure parameter horizontal wind T=0.08 S
101	CAB2	-	1	CROSS Structure parameter horizontal wind T=0.16 S
102	CAB4	-	1	CROSS Structure parameter horizontal wind T=0.32 S
103	CBB1	-	1	Structure parameter BSON T=0.08 S
104	CBB2	-	1	Structure parameter BSON T=0.16 S
105	CBB4	-	1	Structure parameter BSON T=0.32 S
106	CWW1	-	1	Structure parameter vertical wind T=0.08 S
107	CWW2	-	1	Structure parameter vertical wind T=0.16 S
108	CWW4	-	1	Structure parameter vertical wind T=0.32 S
109	CSS1	-	1	Structure parameter TSON T=0.08 S
110	CSS2	-	1	Structure parameter TSON T=0.16 S
111	CSS4	-	1	Structure parameter TSON T=0.32 S
112	CTT1	-	1	Structure parameter PT50 T=0.08 S
113	CTT2	-	1	Structure parameter PT50 T=0.16 S
114	CTT4	-	1	Structure parameter PT50 T=0.32 S
115	CTQ1	-	1	Cross Structure parameter temp and moist T=0.08 S
116	CTQ2	-	1	Cross Structure parameter temp and moist T=0.16 S
117	CTQ4	-	1	Cross Structure parameter temp and moist T=0.32 S
118	CQQ1	-	1	Structure parameter moisture T=0.16 S
119	CQQ2	-	1	Structure parameter moisture T=0.16 S
120	CQQ4	-	1	Structure parameter moisture T=0.32 S
121	DQDV	g/Kg/V	1	Tangent of calibration curve at workpoint Ly-a
122	V0LN	V	1	Shift of calibration curve Ly-a
123	NRAIN	0	1	Fraction of wet samples rain indicator
124	ROTRB	o	3	Rotor begin position
125	ROTRE	o	4	Rotor end position
126	DELT	K	1	Summed temperature differences thermo-couple system
127	T0	K	1	Temperature level 0
128	T1	K	1	Temperature level 1
129	TPOT21	K	1	Potential temperature difference level 2-1
130	TPOT32	K	1	Potential temperature difference level 3-2
131	TPOT43	K	1	Potential temperature difference level 4-3
132	TN0	oC	1	Dewpoint temperature level 0
133	TN1	oC	1	Dewpoint temperature level 1
134	Q0	g/Kg	1	Specific moisture level 0
135	Q1	g/Kg	1	Specific moisture level 1
136	Q21	g/Kg	1	Specific moisture difference level 2-1
137	Q32	g/Kg	1	Specific moisture difference level 3-2
138	Q43	g/Kg	1	Specific moisture difference level 4-3
139	TDEW0	oC	1	Dewpoint level 0
140	TDEW1	oC	1	Dewpoint level 1
141	QDEF	g/Kg	1	Specific moisture deficit
142	THEIM	oC	1	Infrared radiation temperature tree crowns

143	US4	m/s	1	Wind speed level 4 overspeeding corrected
144	US3	m/s	1	Wind speed level 3 overspeeding corrected
145	US2	m/s	1	Wind speed level 2 overspeeding corrected
146	US1	m/s	1	Wind speed level 1 overspeeding corrected
147	UC30U	m/s	1	SQRT(U30^2+VAR(U30)) INTERP->SONIC level
148	UC30C	m/s	1	SQRT(U30^2+VAR(U30)) INTERP->SONIC level OVERSP.CORR
149	U43	m/s	1	U4-U3 with VV correction
150	U32	m/s	1	U3-U2 with VV correction
151	U21	m/s	1	U2-U1 with VV correction
152	UCUP43	m/s	1	Wind speed difference level 4-3
153	UCUP32	m/s	1	Wind speed difference level 3-2
154	UCUP21	m/s	1	Wind speed difference level 2-1
155	USTPR	m/s	1	Friction velocity from profile level 4-2
156	HPR	W/m2	1	Sensible heatflux from profile level 4-2
157	LEPR	W/m2	1	Latent heatflux from profile level 4-2
158	HLEPR	W/m2	1	Total heatflux from profile level 4-2
159	BWPR	0	1	Bowen ratio from profile
160	KSIPR	0	1	Stability (Z-D)/L from profile level 4-2
161	FCPR	m/sppm	1	CO2 flux from from difference in profile
162	GLOBCL	W/m2	1	Clear sky shortwave incoming radiation
163	QNCORR	W/m2	1	QNET corrected for tilt
164	QAIV	W/m2	1	Available energy
165	GBIO	W/m2	1	Heat flux into the biomass
166	GAIR	W/m2	1	Total heat flux into the air column Z<30M
167	FFSU	m/s	1	Wind speed sonic
168	FFSN	m/s	1	Wind speed sonic transducer corrected
169	FFSU30	m/s	1	SQRT(FF^2+uu+vv)
170	FFSN30	m/s	1	SQRT(FF^2+uu+vv) transducer corrected
171	DDSU	o	5	Wind direction sonic
172	DDSN	o	5	Wind direction sonic transducer corrected
173	DLDDSU	o	1	Wind angle relative to sonic frame
174	DLDDSN	o	1	Wind angle relative to sonic frame transducer corrected
175	UU_4	(m/s)2	1	UU , transducer response corrected
176	UU_3	(m/s)2	1	UU_4, along streamline
177	UV_4	(m/s)2	1	UV , transducer response corrected
178	UV_3	(m/s)2	1	UV_3, along streamline
179	UW_5	(m/s)2	1	UW , WSON-jump corrected
180	UW_4	m2/s2	1	UW_5, transducer corrected
181	UW_3	m2/s2	1	UW_4, along streamline
182	US_4	Km/s	1	US , transducer corrected
183	US_3	Km/s	1	US_4, along streamline transducer
184	US_1	Km/s	1	US_3, jump and moisture corrected
185	UT_4	Km/s	1	UT , transducer corrected
186	UT_3	Km/s	1	UT_4, along streamline transducer
187	UQ_4	gm/Kgs	1	UQ , transducer corrected
188	UQ_3	gm/Kgs	1	UQ_4, along streamline transducer
189	UQ_1	gm/Kgs	1	UQ_3, temperature corrected
190	VV_4	(m/s)2	1	VV , transducer response corrected
191	VV_3	(m/s)2	1	VV_4, along streamline
192	VW_5	(m/s)2	1	VW , WSON-jump corrected
193	VW_4	m2/s2	1	VW_5, transducer corrected
194	VW_3	m2/s2	1	VW_4, along streamline
195	VS_4	Km/s	1	VS , transducer corrected
196	VS_3	Km/s	1	VS_4, along streamline transducer
197	VS_1	Km/s	1	VS_3, jump and moisture corrected
198	VT_4	Km/s	1	VT , transducer corrected
199	VT_3	Km/s	1	VT_4, along streamline transducer
200	VQ_4	Km/s	1	VQ , transducer corrected
201	VQ_3	Km/s	1	VQ_4, along streamline transducer
202	VQ_1	Km/s	1	VQ_3, temperature corrected
203	WW_5	(m/s)2	1	WW , WSON-jump corrected
204	WW_4	m2/s2	1	WW_5, transducer corrected
205	WW_3	m2/s2	1	WW_4, along streamline
206	WS_5	km/s	1	WS , WSON-jump corrected
207	WS_4	Km/s	1	WS_5, transducer corrected
208	WS_3	Km/s	1	WS_4, along streamline transducer
209	WB	Km/s	1	WS_3, jump corrected
210	WS_2	Km/s	1	WS_3, jump and moisture corrected (LEMD)
211	WS_1	Km/s	1	WS_3, jump and moisture corrected (LYAL)
212	WT_5	Km/s	1	WT , WSON-jump corrected
213	WT_4	Km/s	1	WT_5, transducer corrected
214	WT_3	Km/s	1	WT_4, along streamline transducer
215	WQ_5	gm/Kgs	1	WQ , WSON-jump correctedI
216	WQ_4	Km/s	1	WQ_5, transducer corrected
217	WQ_3	Km/s	1	WQ_4, along streamline transducer
218	WQ_2	Km/s	1	WQ_5, temperature corrected
219	WQ_1	Km/s	1	WQ_3, temperature corrected
220	SS_1	K2	1	SS , jump and moisture corrected
221	ST_1	K2	1	ST , jump and moisture corrected
222	SQ_1	gK/Kg	1	SQ , jump,moisture and temperature corrected
223	TQ_1	gK/Kg	1	TQ , temperature corrected
224	QQ_1	g2/Kg2	1	QQ , temperature corrected
225	USTUN	m/s	2	SQRT(-UW_1)
226	USTER	m/s	1	SQRT(-UW_3)

227	USTABS	m/s	1	U* from Length stress vector, UW and VW
228	TSTER	K	1	Turbulence temperature scale, WS and USTER
229	QSTER	g/Kg	1	Turbulence moisture scale, WQ and USTER
230	HSON	W/m2	1	Sensible heat flux from WS
231	HED	W/m2	1	Sensible heat flux from WT
232	LEED	W/m2	1	Latent heat flux from WQ
233	HLEED	W/m2	1	Total turbulence heat flux
234	BWED	0	1	Bowen ratio eddy-correlation
235	LOBH	m	1	Obukhov length
236	KSIED	1/m	1	Inverse of Obukhov length eddy correlation
237	LEBWSN	W/m2	1	Latent heatflux from HSON and BWPR
238	HBW	W/m2	1	Sensible heat from QAIV EN BWPR
239	LEBW	W/m2	1	Latent heat from QAIV and BWPR
240	LEMD	W/m2	1	Latent heat Single-big-leaf-model (Bosveld,1991)
241	LEBAL	W/m2	1	Latent heat from energy balance with HSON
242	LEEQ	W/m2	1	Equillibrium evaporation
243	CWW1_5	-	1	CWW1 , WSON-jump corrected
244	CWW1_1	-	1	CWW1_5, line averaging corrected
245	CWW2_5	-	1	CWW2 , WSON-jump corrected
246	CWW2_1	-	1	CWW2_5, line averaging corrected
247	CWW4_5	-	1	CWW4 , WSON-jump corrected
248	CWW4_1	-	1	CWW4_5, line averaging corrected
249	CWW	-	1	Average over CWW2_1 and CWW4_1
250	WWC	-	1	WW_3, line averaging corrected
251	CNN	-	1	SQRT of refraction index Structure parameter
252	YSON_4	m/s	1	YSON , transducer response corrected
253	XSON_4	m/s	1	XSON , transducer response corrected
254	WSON_4	m/s	1	WSON , tilted W-SENSOR corrected
255	WSON_3	m/s	1	WSON_4, relative to horizontal plane
256	ELEV	o	1	Elevation of the stream line
257	AZWAT	o	1	Azimuth of inclinometer vector
258	FFWAT	o	1	Length of inclinometer vector
259	K_DIR	W/m2	1	Direct solar radiation from De Jong model
260	ELSOL	rad	1	Solar elevation
261	AZSOL	rad	1	Solar azimuth
262	GDIR	W/m2	1	Direct solar radiation from Raaf model
263	GDIFF	W/m2	1	Diffuse solar radiation from Raaf model
264	CWWD	m/s	1	CWW from difference CWW4_1 and CWW1_1
265	U1	m/s	0	Vector jumpspeed level 1 derived from US1
266	U2	m/s	0	Vector jumpspeed level 1 derived from US1
267	U3	m/s	0	Vector jumpspeed level 1 derived from US1
268	U4	m/s	0	Vector jumpspeed level 1 derived from US1
269	LEPOT	W/m2	0	Potential evaporation
270	UMAX	-	7	-
271	UMIN	-	8	-
272	UVAR	-	0	-
273	DTMAX	-	7	-
274	DTMIN	-	8	-
275	DTVAR	-	0	-
276	TEND	-	4	-
277	TBEG	-	3	-
278	TVAR	-	0	-
279	DDEND	-	4	-
280	DDBEG	-	3	-
281	DDVAR	-	0	-
282	RIVGT1	-	0	Richardson number forest interior T1-t0/u1^2
283	RIVGTH	-	0	Richardson number forest interior THEIM-t0/u1^2
284	GAIRS	-	1	Sensible heat flux stored between 15 and 30m
285	GAIRL	-	1	Latent heat flux stored between 15 and 30m
286	VARB	K2	1	Sonic temperature variance, jump corrected
287	TCONV	K	1	Convective temperature scale, stability corrected
288	ZNULVL	m	0	Displacement height
289	Zsonic	m	0	Height of sonic anemometer
290	ZT4	m	0	Height of temperature level 4
291	ZT3	m	0	Height of temperature level 3
292	ZT2	m	0	Height of temperature level 2
293	ZT1	m	0	Height of temperature level 1
294	ZT0	m	0	Height of temperature level 0
295	ZU4	m	0	Height of jump level 4
296	ZU3	m	0	Height of jump level 3
297	ZU2	m	0	Height of jump level 2
298	ZU1	m	0	Height of jump level 1
299	ZU0	m	0	Height of jump level 0

KNMI-Publicaties, Technische & Wetenschappelijke Rapporten, gepubliceerd sedert 1995

Een overzicht van eerder verschenen publicaties, wordt verzoek toegezonden door de Bibliotheek van het KNMI, postbus 201, 3730 AE De Bilt, tel. 030 - 2 206 855, fax. 030 - 2 210 407; e-mail: biblioth@knmi.nl

▼ KNMI-PUBLICATIE MET NUMMER

150-28 Sneeuwdek in Nederland 1961-1990 / A.M.G. Klein Tank

176-S Stormenkalender: chronologisch overzicht van alle stormen (windkracht 8 en hoger) langs de Nederlandse kust voor het tijdvak 1990-1996 / [samenst. B. Zwart ea.]

180a List of acronyms in environmental sciences : revised edition / [compiled by P. Geerders and M. Waterborg]

181a FM12 SYNOP · internationale en nationale regelgeving voor het coderen van de groepen 7wwW1W2 en 960ww

181b FM12 SYNOP · internationale en nationale regelgeving voor het coderen van de groepen 7wwW1W2 en 960ww; derde druk

183-1 Rainfall in New Guinea (Irian Jaya) / T.B. Ridder

183-2 Vergelijking van zware regens te Hollandia (Nieuw Guinea), thans Jayapura (Irian Jaya) met zware regens te De Bilt / T. B. Ridder

183-3 Verdamping in Nieuw-Guinea, vergelijking van gemeten hoeveelheden met berekende hoeveelheden / T.B. Ridder

183-4 Beschrijving van het klimaat te Merauke, Nieuw Guinea, in verband met de eventuele vestiging van een zoutwinningsbedrijf / T.B. Ridder ea.

183-5 Overzicht van klimatologische en geofysische publikaties betreffende Nieuw-Guinea / T.B. Ridder

184 Inleiding tot de algemene meteorologie : studie-uitgave / B. Zwart, A. Steenhuisen, m.m.v. H.J. Krijnen

184a Inleiding tot de algemene meteorologie : studie-uitgave ; 2e, druk / B. Zwart, A. Steenhuisen, m.m.v. H.J. Krijnen

185 Handleiding voor het gebruik van sectie 2 van de FM 13-X SHIP-code door stations op zee / KNMI; KLu; KM

185a Handleiding voor het gebruik van sectie 2 van de FM 13-X SHIP-code voor waarnemers op zee / KNMI; KLu; KM

186-I Rainfall generator for the Rhine Basin: single-site generation of weather variables by nearest-neighbour resampling / T. Brandsma and T.A. Buishand

187 De wind in de rug: KNMI-weerman schaatst de Elfstedentocht / Henk van Dorp

▼ TECHNISCH RAPPORT = TECHNICAL REPORT (TR)

168 Analyse van het seismische risico in Noord-Nederland / Th. de Crook, B. Dost en H.W. Haak

173 Measurement of the structure parameter of vertical wind-velocity in the atmospheric boundary layer / R. van der Ploeg

174 Report of the ASGASEX'94 workshop / ed. by W.A. Oost

175 Over slecht zicht, bewolking, windstoten en gladheid / J. Terpstra

176 Verification of the WAQUA/CSM-16 model for the winters 1992-93 and 1993-94 / J.W. de Vries

177 Nauwkeuriger nettostraling meten / M.K. van der Molen en W. Kohsiek

178 Neerslag in het stroomgebied van de Maas in januari 1995: waarnemingen en verificatie van modelprognoses / R.Jilderda ea.

179 First field experience with 600PA phased array sodar / H. Klein Baltink

180 Een Kalman-correctieschema voor de wegdektemperatuurverwachtingen van het VAISALA-model / A. Jacobs

181 Calibration study of the K-Gill propeller vane / Marcel Bottema

182 Ontwikkeling van een spectraal UV-meetinstrument / Frank Helderman

183 Rainfall generator for the Rhine catchment : a feasibility study / T. Adri Buishand and Theo Brandsma

184 Parametrisatie van mooi-weer cumulus / M.C. van Zanten

185 Interim report on the KNMI contributions to the second phase of the AERO-project / Wiel Wauben, Paul Fortuin ...[et al.]

186 Seismische analyse van de aardbevingen bij Middelstum (30 juli 1994) en Annen (16 augustus '94 en 31 januari '95) / [SO]

187 Analyse wenselijkheid overname RIVM-windmeetlokaties door KNMI / H. Benschop

188 Windsnelheidsmetingen op zeestations en kuststations: herleiding waarden windsnelheden naar 10-meter niveau / H. Benschop

189 On the KNMI calibration of net radiometers / W. Kohsiek

190 NEDWAM statistics over the period October 1994 - April 1995 / F.B. Koek

191 Description and verification of the HIRLAM trajectory model / E. de Bruijn

192 Tiltmeting . een alternatief voor waterpassing ? / H.W. Haak

193 Error modelling of scatterometer, in-situ and ECMWF model winds; a calibration refinement / Ad Stoffelen

194 KNMI contribution to the European project POPSICLE / Theo Brandsma and T. Adri Buishand

195 ECBILT . a coupled atmosphere ocean sea-ice model for climate predictability studies / R.J. Haarsma ao.

196 Environmental and climatic consequences of aviation: final report of the KNMI contributions to the AERO-project / W. Wauben ao.

197 Global radiation measurements in the operational KNMI meteorological network: effects of pollution and ventilation / F. Kuik

198 KALCORR: a kalman-correction model for real-time road surface temperature forecasting / A. Jacobs

199 Macroseismische waarnemingen Roswinkel 19-2-1997 / B. Dost en H.W Haak

200 Operationele UV-metingen bij het KNMI / F. Kuik

201 Vergelijking van de Vaisala's HMP233 en HMP243 relatieve luchtvochtigheidsmeters / F. Kuik

202 Statistical guidance for the North Sea / Janet Wijngaard and Kees Kok

203 UV-intercomparison SUSPEN / Foeke Kuik and Wiel Wauben

204 Temperature corrections on radiation measurements using Modtran 3 / D.A. Bunskoek, A.C.A.P. van Lammeren and A.J. Feijt

205 Seismisch risico in Noord-Nederland / Th. De Crook, H.W. Haak en B. Dost

206 The HIRLAM-STAT-archive and its application programs / Albert Jacobs

207 Retrieval of aerosol properties from multispectral direct sun measurements / O.P. Hasekamp

▼ WETENSCHAPPELIJK RAPPORT = SCIENTIFIC REPORT (WR)

95-01 Transformation of precipitation time series for climate change impact studies / A.M.G. Klein Tank and T.A. Buishand

95-02 Internal variability of the ocean generated by a stochastic forcing / M.H.B. van Noordenburg

95-03 Applicability of weakly nonlinear theory for the planetary-scale flow / E.A. Kartashova

95-04 Changes in tropospheric NOx and O3 due to subsonic aircraft emissions / W.M.F. Wauben ao.

95-05 Numerical studies on the Lorenz84 atmosphere model / L.Anastassiades

95-06 Regionalisation of meteorological parameters / W.C. de Rooy

95-07 Validation of the surface parametrization of HIRLAM using surface-based measurements and remote sensing data / A.F. Moene ao.

95-08 Probabilities of climatic change : a pilot study / Wieger Fransen (ed.) and Alice Reuvekamp

96-01 A new algorithm for total ozone retrieval from direct sun measurements with a filter instrument / W.M.F. Wauben

96-02 Chaos and coupling: a coupled atmosphere ocean-boxmodel for coupled behaviour studies / G. Zondervan

96-03 An acoustical array for subsonic signals / H.W. Haak

96-04 Transformation of wind in the coastal zone / V.N. Kudryavtsev and V.K. Makin

96-05 Simulations of the response of the ocean waves in the North Atlantic and North Sea to CO2 doubling in the atmosphere / K Rider ao.

96-06 Microbarograph systems for the infrasonic detection of nuclear explosions / H.W. Haak and G.J. de Wilde

96-07 An ozone climatology based on ozonesonde measurements / J.P.F. Fortuin

96-08 GOME validation at KNMI and collaborating institutes / ed. by P Stammes and A. Piters

97-01 The adjoint of the WAM model / H. Hersbach

97-02 Optimal interpolation of partitions: a data assimilation scheme for NEDWAM-4; description and evaluation of the period November 1995 - October 1996 / A.Voorrips

97-03 SATVIEW: a semi-physical scatterometer algorithm / J.A.M. Janssen and H. Wallbrink

97-04 GPS water vapour meteorology : status report / H. Derks, H. Klein Baltink, A. van Lammeren, B. Ambrosius, H. van der Marel ao.

97-05 Climatological spinup of the ECBILT oceanmodel / Arie Kattenberg and Sybren S. Drijfhout

97-06 Direct determination of the air-sea transfer velocity of CO2 during ASGAMAGE / J.C.M. Jacobs, W. Kohsiek and W.A. Oost

97-07 Scattering matrices of ice crystals / M. Hess, P. Stammes and R.B.A. Koelemeijer

97-08 Experiments with horizontal diffusion and advection in a nested fine mesh mesoscale model / E.I.F. de Bruijn

97-09 On the assimilation of ozone into an atmospheric model / E.Valur Hólm

98-01 Steady state analysis of a coupled atmosphere ocean-boxmodel / F.A. Bakker

98-02 The ASGAMAGE workshop, September 22-25, 1997 / ed. W.A. Oost

98-03 Experimenting with a similarity measure for atmospheric flows / R.A. Pasmanter and X.-L. Wang

98-04 Evaluation of a radio interferometry lightning positioning system / H.R.A. Wessels